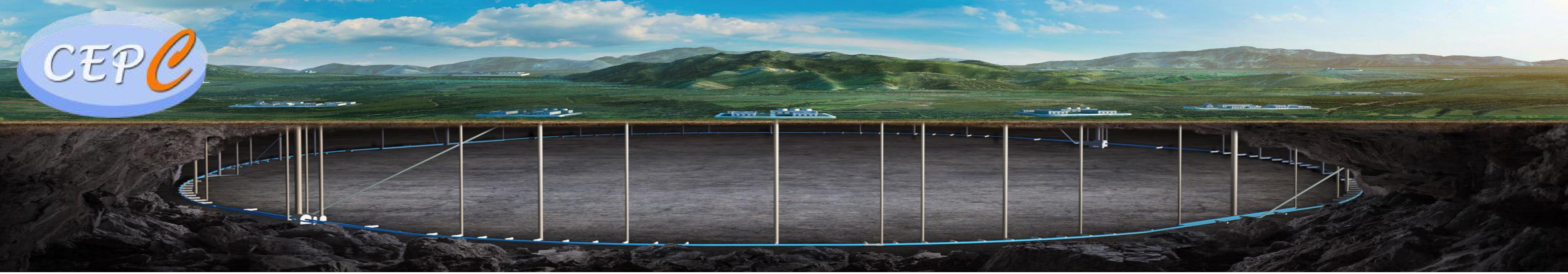

TDR Editor Report

Including checking:
- Implementation of IDRC comments
- Format check (tables, figures…)

中国科学院高能物理研究所
Institute of High Energy Physics
Chinese Academy of Sciences

Chapter Editors

2 Concept of CEPC Reference Detector	Mingshui
3 MDI and Luminosity Measurement	Manqi
4 Vertex Detector	Mingyi
5 Silicon Trackers	Jingbo
6 Pixelated Time Projection Chamber	Mingyi
7 Electromagnetic calorimeter	Manqi
8 Hadronic calorimeter	Jianbei
9 Muon Detector	Miao He
10 Detector magnet system	Haijun
11 Readout Electronics	Zheng
12 Trigger and Data Acquisition	Zheng
13 Offline software and computing	Gang
14 Mechanics and integration	Jingbo
15 Detector and physics performance	Weidong

HADRONIC CALORIMETER

Findings

- A key innovative feature of the Hadronic Calorimeter (HCAL) is the large sampling fraction achieved through the use of heavy scintillating glasses (GS). The proposed layout offers the potential to significantly improve the PFA resolution by enhancing the stochastic term of the single-particle energy resolution. The committee acknowledges that the team is highly motivated and is making steady progress toward this ambitious design.

Findings

- The proposal is reasonable but aggressive. Detector specifications and performance benchmarks are clearly defined; however, considerable work is needed to bring the GS-HCAL baseline choice from its current R&D phase to a full-scale detector.

- --The primary objective of this section is to validate that the GS-HCAL design meets the CEPC physics program's core performance criteria. Leveraging extensive simulation studies in the absence of prototype data, we demonstrate the design's compliance with these requirements. In the new version in **Section 8.5 (** simulation and performance).

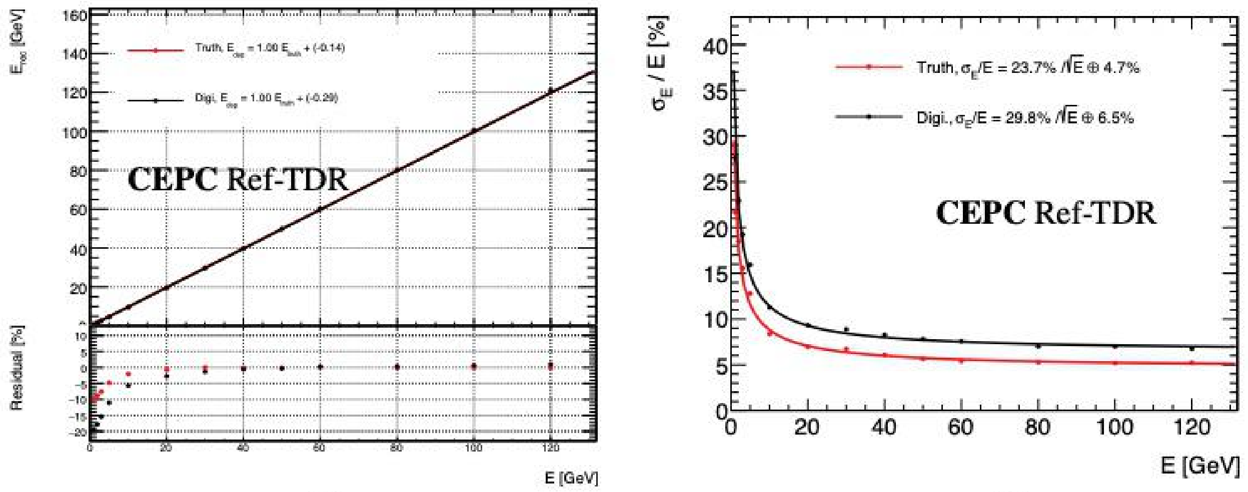

(a) (b)

Figure 8.24: (a) Energy linearity and (b) energy resolution of GS-HCAL with the digitization model.

The estimated energy resolution of $\sigma E/E$ = 29.8%/$\sqrt{E}$ ⊕ 6.5% and an energy linearity within 2% before calibration, outperforms the stochastic term of traditional HCALs.

Findings

- For instance, during the review, the team was uncertain about the origin of the constant term observed in the hadronic energy resolution, a result obtained from idealized simulations with only limited hardware effects included.

- --To verify the hypothesis that longitudinal leakage was the cause of the observed discrepancy, we increased the depth of the GS-HCAL from 48 layers (6 λ_I) to 80 layers (10 λ_I) in **Section 8.5.2 Hadron Energy Resolution**. When the calorimeter depth was extended to 80 layers, this tail decreased significantly, and the constant term dropped to around 2.9%. The significant improvement in the constant term upon increasing the depth of the GS-HCAL supported the hypothesis that shower leakage, rather than an intrinsic design flaw.

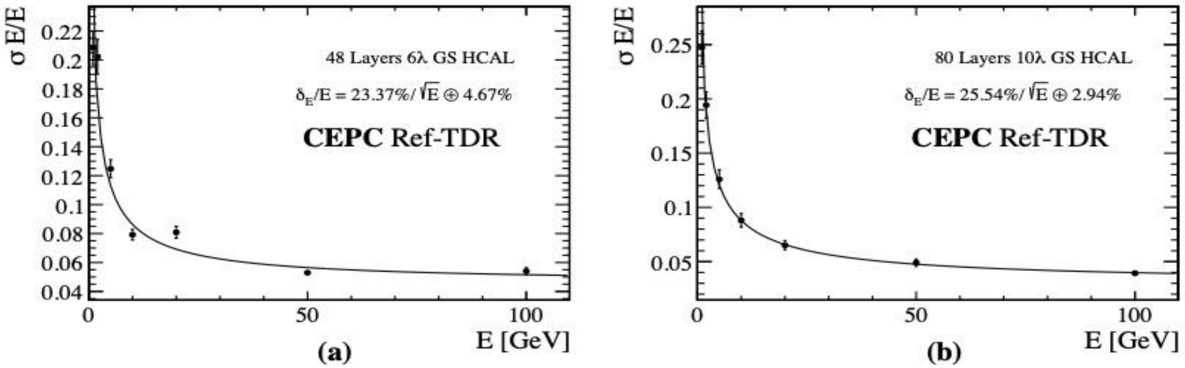

Figure 8.27: Comparison of two GS-HCAL configurations with different depths. A shallower setup with 6 λ_I (a) yields a pronounced high tail in the energy resolution and a large constant term. A deeper setup with 10 λ_I (b) effectively contains the showers, reducing the tail and lowering the constant term to a more typical value.

Findings

- The committee is pleased to note that the next step is the construction of a large-scale prototype.

- --Yes, in the new version of the HCAL-TDR, the new design of the prototype has already described, as in the **Section 8.4.8 Prototype**. The construction and testing program proceeds in phases. A 3×3×7 mini-prototype is currently under construction for initial beam tests at CERN in October 2025. The full 8112-channel prototype is scheduled for completion by end-2026.

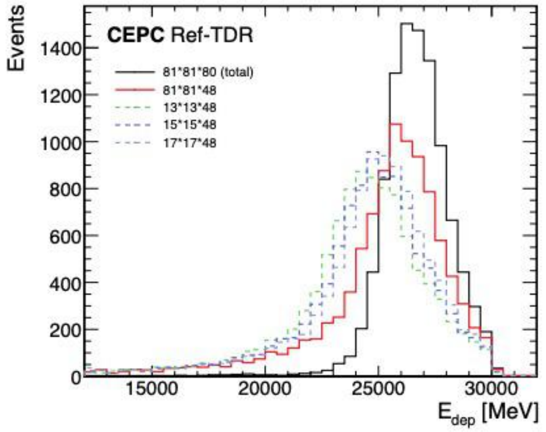

Figure 8.22: Distribution of deposited energy in prototype with different size using 80 GeV π for simulation.

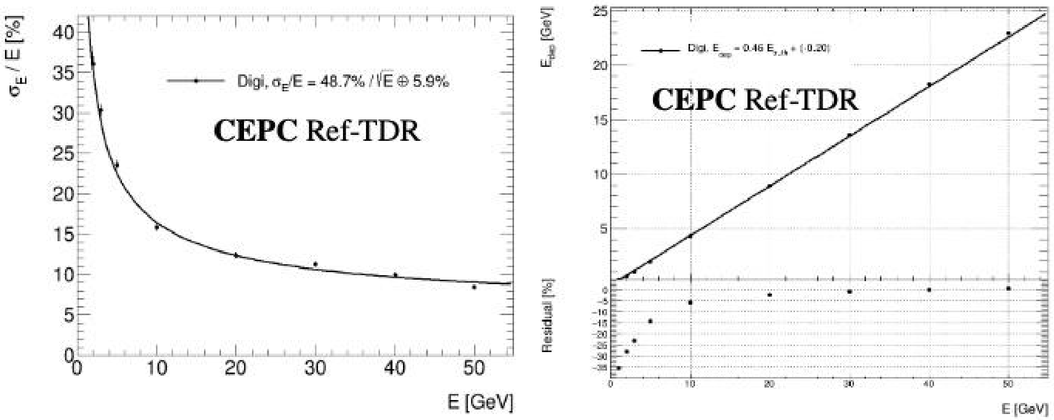

(a) (b)

Figure 8.23: (a) Energy resolution and (b) energy linearity of GS-HCAL prototype based on simulation.

Findings

- In this prototype, each tile will be read out by four SiPMs, whereas in the final detector only one SiPM per tile is foreseen for cost reasons.

- --It is clear that there is only one SiPM for tile for the design and cost, as show in **Figure 8.2**, and detialed describe could be found in **section 8.2.1** (Single layer structure). In the **Section 8.4.5** (Measurements of GS with SiPM), it is shown the cosmic ray test result of the 4cm*4cm*1cm glass cell coupling with 1 piece of 3mm*3mm SiPM.

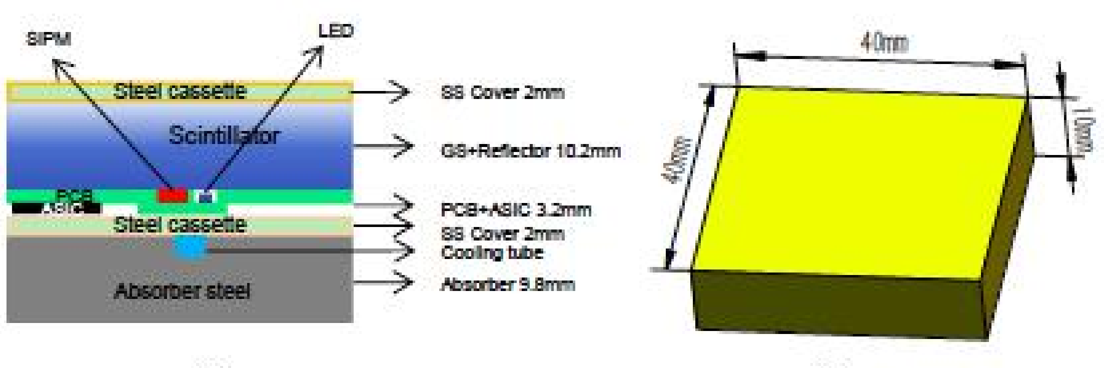

(a) (b)

Figure 8.2: (a) Single layer structure of GS-HCAL. (b) One GS cell.

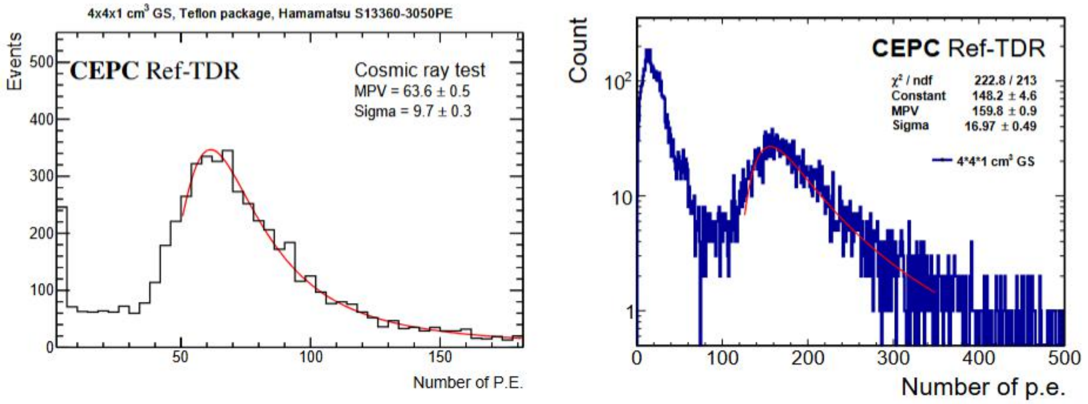

(a) (b)

Findings

HCAL

- Regarding costs, the committee notes that the current cost estimate does not include the cost of PCBs, which experience shows can become a significant item for granular calorimeters due to the complexity of design and production.

- --the cost of PCBs has already included in the electronics part.

Findings

- It was also acknowledged that a sampling calorimeter based on plastic scintillator (PS-AHCAL), which is more mature and better understood, remains a viable fallback option. The committee encourages the team to continue pursuing the GS-HCAL option, while maintaining the PS-HCAL as a backup.

- --Yes, the GS-HCAL and PS-HCAL are both the options of the HCAL. the size of the GS or PS tile are the same as 4cm*4cm, has the same photon readout SiPM and the electrinics, the same size Box and Prototypes. If the GS R&D was falled, it will be easy go back to the PS-HCAL design. There is also a special **Section 8.6 (**Alternative HCAL options) introduce the R&D results of the RPC-SDHCAL and PS-HCAL.

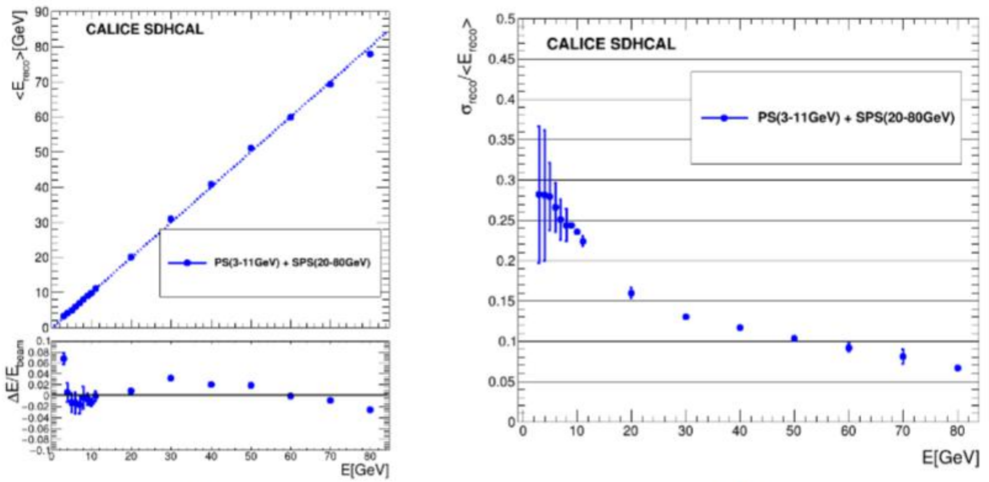

(a) (b)

RPC-SDHCAL

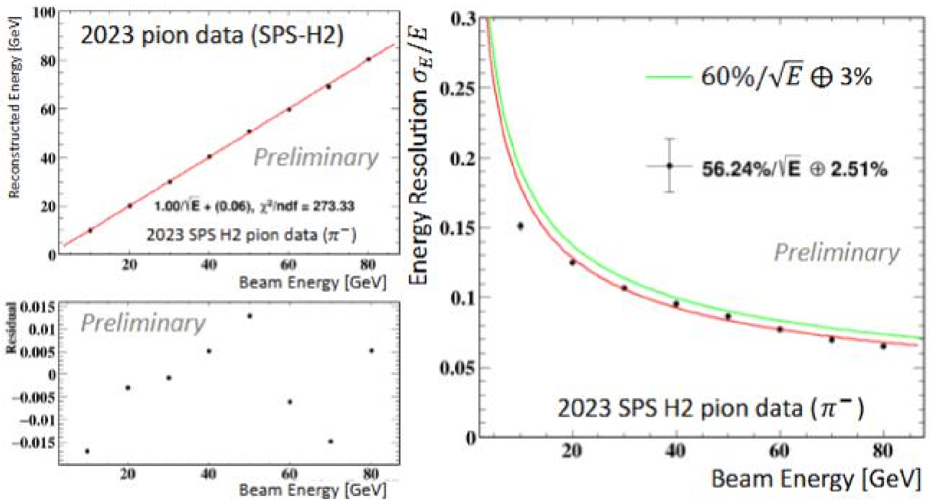

(a) (b)

PS-HCAL

Comments

- Scintillating glasses represent new territory for hadronic calorimetry. The material properties, such as radiation length and hadronic interaction length, are not yet fully characterized. Although the decision to adopt this technology is well justified, it carries significant risk. Therefore, extensive prototyping and simulation studies are mandatory to validate the concept.

- --Yes, the study of the GS-HCAL option is only start in two years ago, and choise to be the baseline option on Aug.2024, there are lots studies need to do. And the new design of the prototype has already described, as in the **Section 8.4.8**.

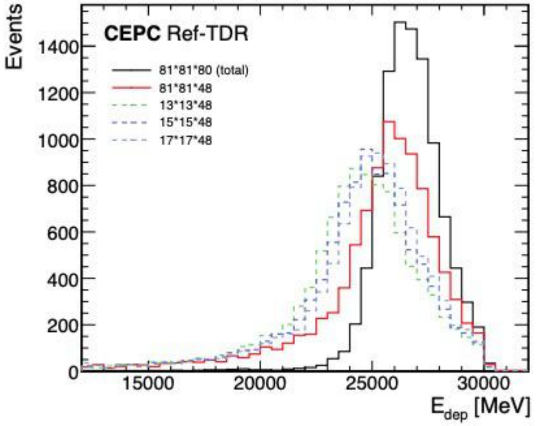

Figure 8.22: Distribution of deposited energy in prototype with different size using 80 GeV π for simulation.

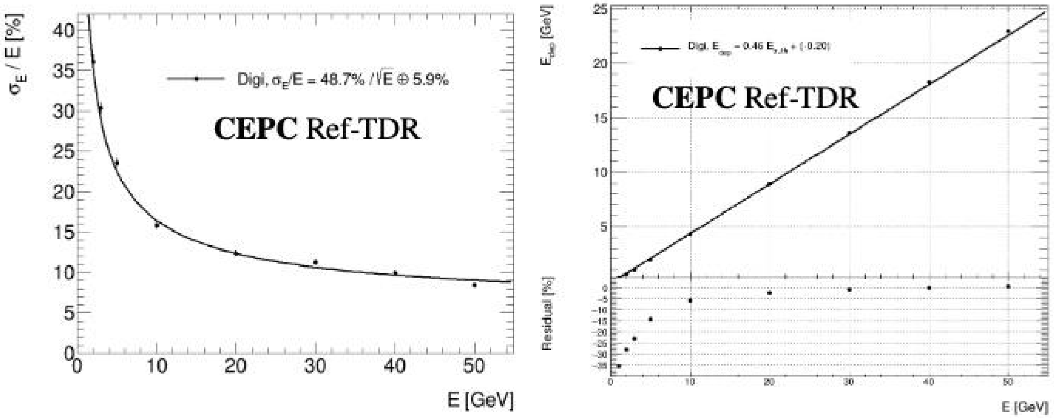

(a) (b)

Figure 8.23: (a) Energy resolution and (b) energy linearity of GS-HCAL prototype based on simulation.

Comments

HCAL

- A deep understanding of the response to hadrons is essential, including clarification of the constant term origin, study of the e/h ratio (software compensation), validation of GEANT4 physics lists, and accurate characterization of material properties such as quenching (Birks' law).

- --The new version of the TDR ahs already update the simulation work and the group also did more study for the design. In **Section 8.5 simulation and performance**. The energy linearity and resolution of the GS-HCAL are estimated using Geant4 simulation within the CEPC Software (CEPCSW) framework.

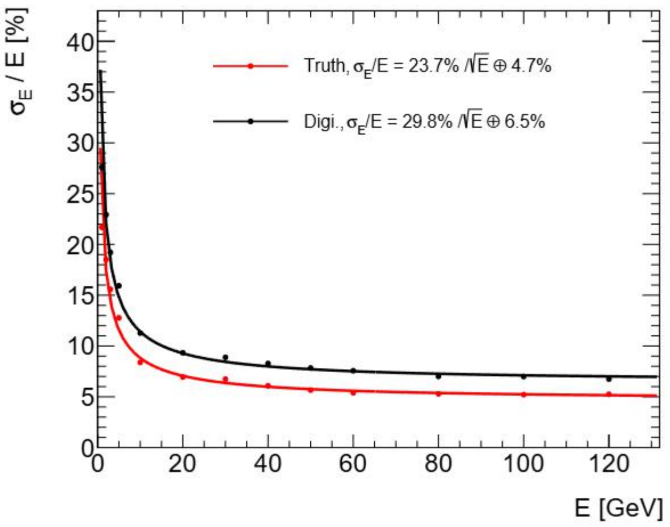

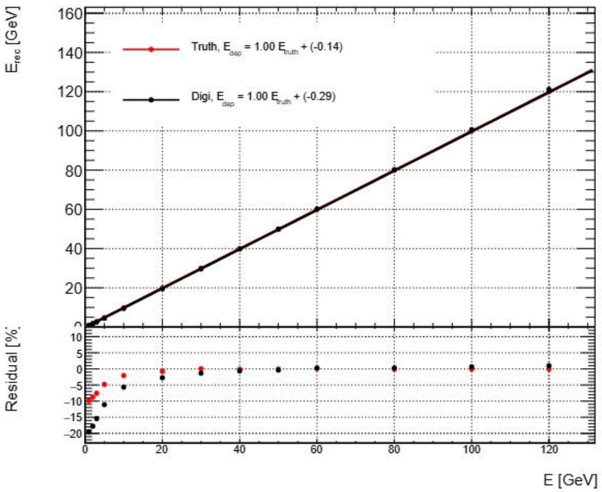

The estimated energy resolution of $\sigma E / E$ = 29.8%/$\sqrt{E}$ $\oplus$ 6.5% and an energy linearity within 2% before calibration, outperforms the stochastic term of traditional HCALs.

Comments

HCAL

- The introduction of the TDR currently lacks references to important developments such as the CALICE AHCAL, built by German, Czech, and Japanese groups, which served as a foundation for the scintillator section of the CMS HGCAL.

- --The refs has already marked in the new version. Especially in the **Section 8.6 (Alternative HCAL options)**, it is introduced the developments of different option for HCAL. Multiple technological approaches of the CEPC calorimeters have been investigated to achieve the required jet energy resolution. These include gaseous detector-based approaches like the Digital HCAL (DHCAL) [29, 30] and SDHCAL [5, 31], as well as plastic scintillator tile designs (AHCAL) [10–13].

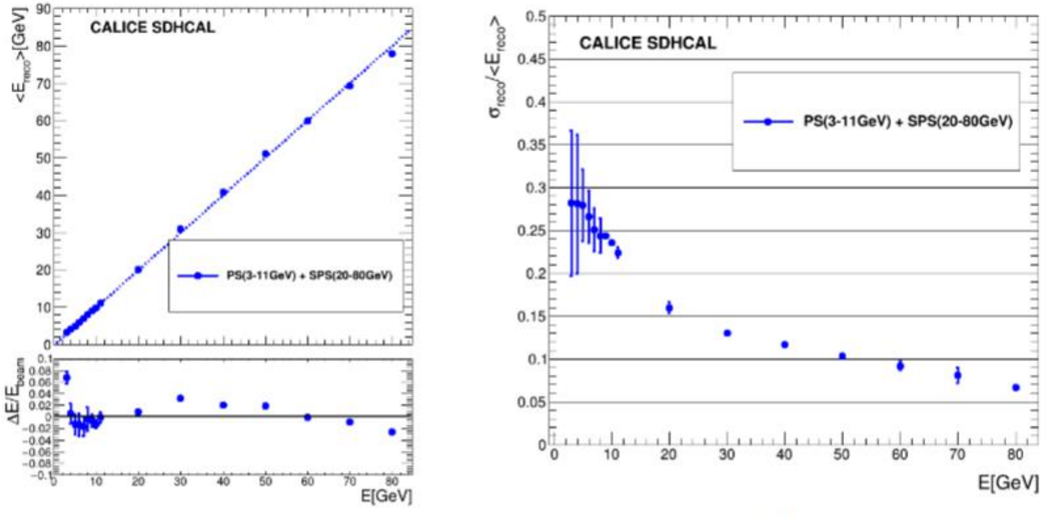

(a) (b)

RPC-SDHCAL

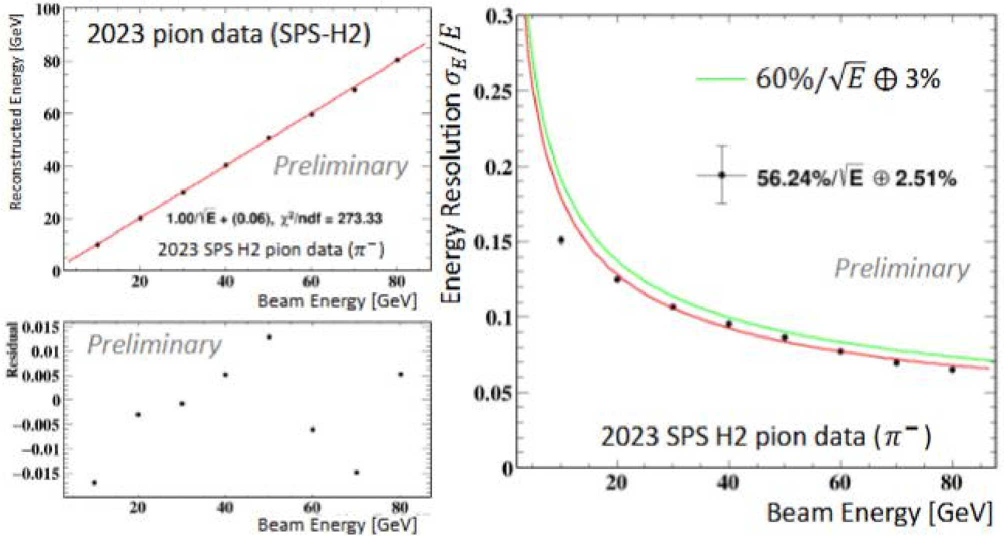

(a) (b)

PS-HCAL

Comments

HCAL

- The process of down-selecting technology options should be better explained in the text. Statements such as "excessive power consumption" should be supported with quantitative arguments for clarity and transparency.

- --The quality of the language has already improved a lot in the new version. In this new version, only one person (Li Hengne) represents the whole HCAL team to write documents and hold discussions with others, maintaining the uniqueness of the writing style.

Recommendations

- Develop a detailed plan to validate the choice of GS-HCAL technology in a timely manner. This plan should include the development of glass samples with reproducible and controlled quality, along with a detailed understanding of single-particle and jet energy resolution.

- --Yes, in the new version, there is a new **section 8.4 (**Technology R&D to demonstrate technologies and prototypes) introduced the technology of HCAL as GS, SiPM, Simulation and Calibration. To verify the performance stability of the GS, a batch of 150 glass samples were produced, and corresponding performance tests were conducted.

- In **Section 8.5.2** （Hadron Energy Resolution）introduce the energy linearity and energy resolution of GS-HCAL with the digitization model.

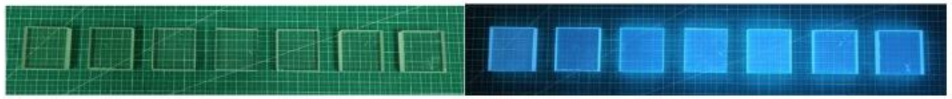

(a) (b)

Figure 8.11: GFO glass cells with the size of $40 \times 40 \times 10$ mm^3 under (a) natural light and (b) ultraviolet light.

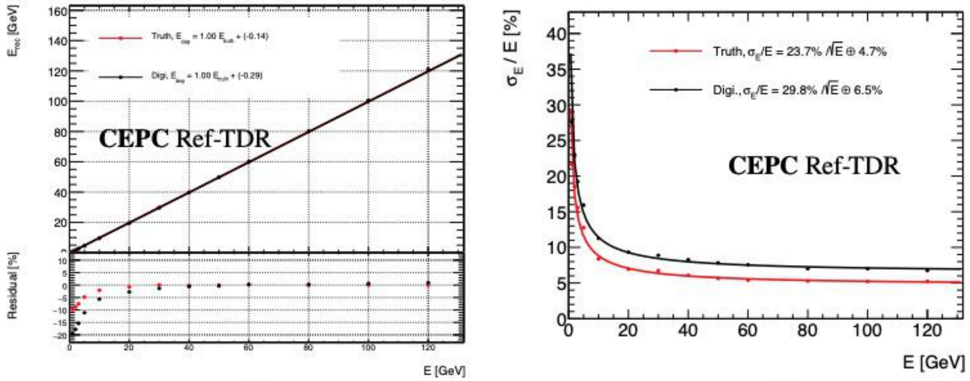

(a) (b)

Figure 8.24: (a) Energy linearity and (b) energy resolution of GS-HCAL with the digitization model.

Recommendations

HCAL

- Prioritize the construction of a full-scale prototype. This prototype should incorporate the preliminary selection of glass tiles and ideally include a first version of both the readout ASIC and the PCB. Decide early on the final configuration regarding the number of SiPMs per tile and implement this choice in the prototype.

- --Good suggestion, the final prototype will use the GS,ASIC and PCBs, which will be used in the HCAL-CEPC in the future. A 3×3×7 mini-prototype is currently under construction for initial beam tests at CERN in October 2025. This mini-prototype will use the DT5202 from CAEN (https://www.caen.it/products/dt5202/)for electronics. But the full 8112-channel prototype scheduled for completion by end-2026, with include the readout ASIC and the PCB by our electronics group in CEPC. The full 8112-channel prototype is scheduled for completion by end-2026, with cosmic ray tests planned at IHEP and subsequent beam tests preferably at CERN in 2027. This prototype implements a steel-scintillator sandwich structure in a compact 0.6 m^3 volume (52 cm × 52 cm × 130.6 cm).

- Organize the group's work such that the prototype is simultaneously implemented into the simulation framework, including a complete digitization chain, to enable rapid feedback from test beam campaigns.

- --Yes, These will be the next steps to focus on.

The Mini-Prototype for beam tests at CERN in October 2025

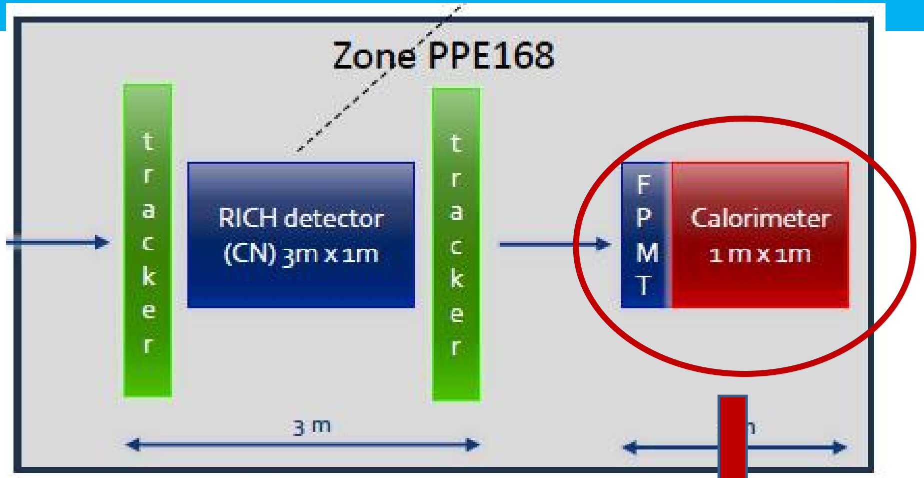

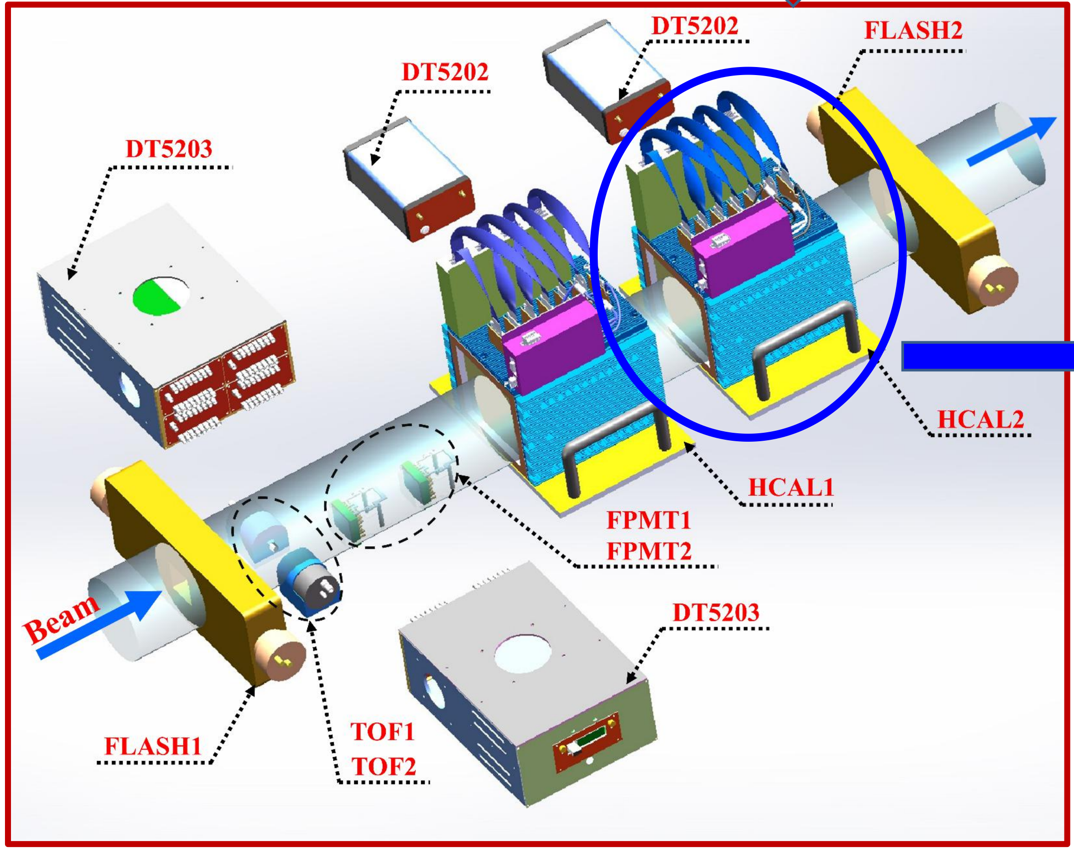

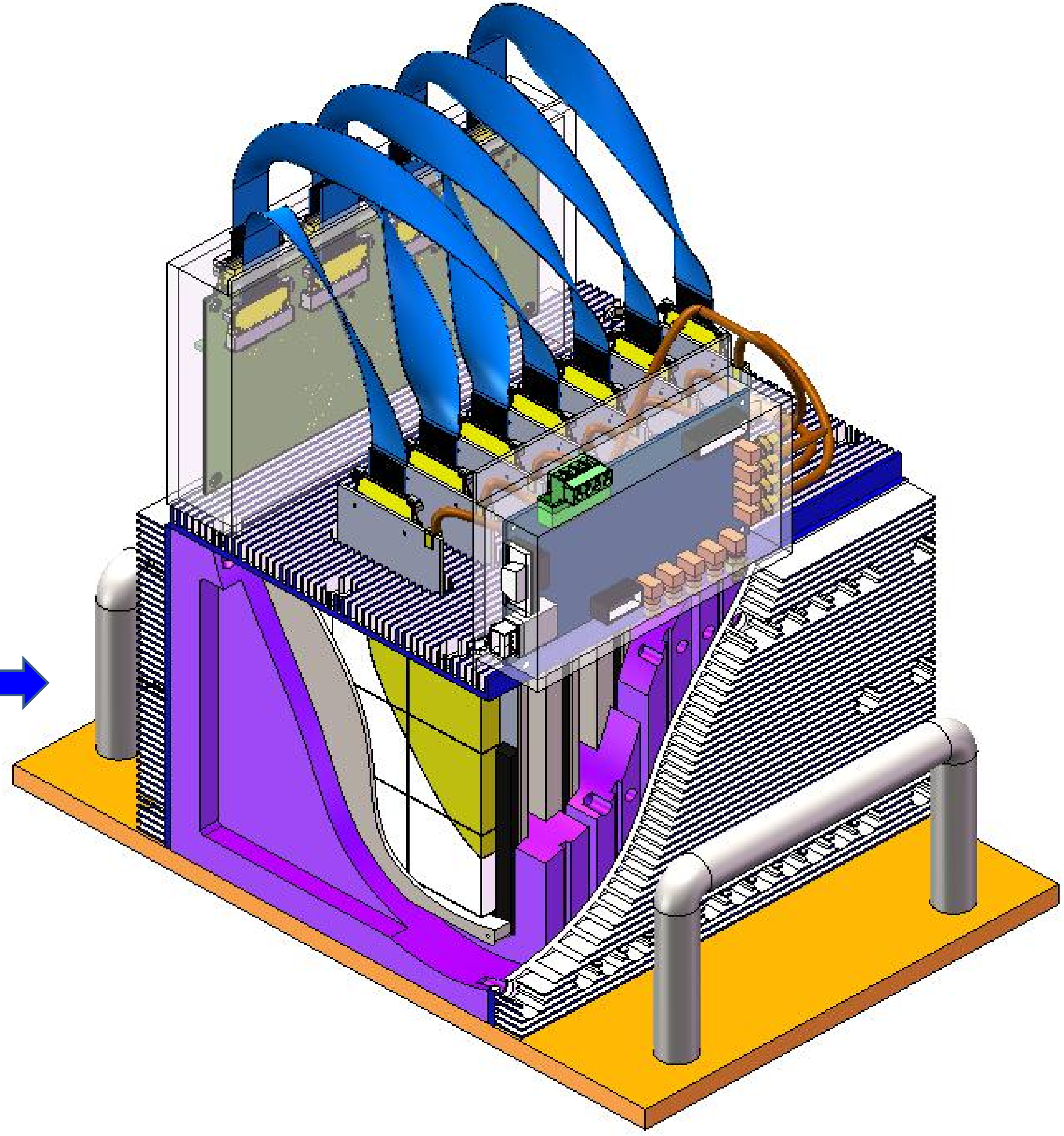

Comments in backup

- The authors are encouraged to make the text more concise where possible, while still providing sufficient detail where necessary.
  - o Captions such as that for Fig. 8.12 ("The real AHCAL prototype") are inadequate and should be made more informative.

--the outline of the HCAL in new version has changed, this types of pictures were deleted.

  - o The authors should carefully review the text to ensure that all figures are properly motivated, and that the overall argumentation is logical and coherent.

--the outline of the HCAL in new version has changed.

  - o For example, it is unclear why the emission spectrum shown in Fig. 8.52 is included—is it representative or used for digitization? This should be explicitly explained.

--this figure was deleted. Totally about 91 figures aere deleted, and all the figures in the new version TDR were modfied with high quality.

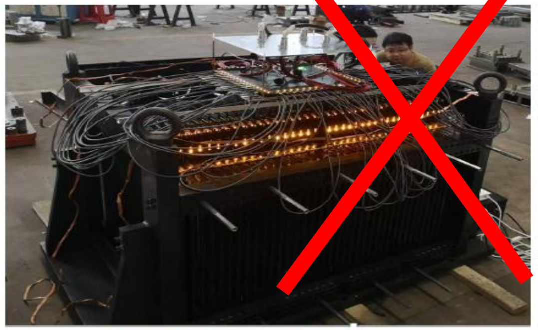

Figure 1.12: The real AHCAL prototype.

Fig. 8.12 in old version

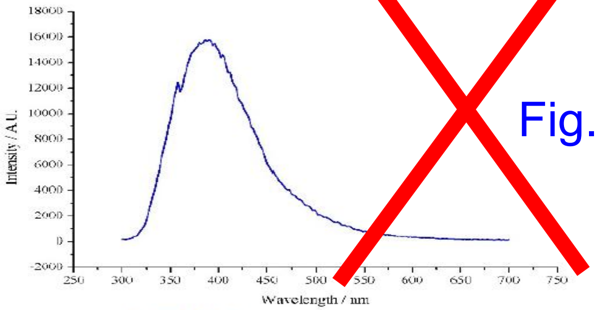

Figure 1.52: The emission spectrum of GS.

Fig. 8.52 in old version

Comments in backup

HCAL

- The authors are encouraged to make the text more concise where possible, while still providing sufficient detail where necessary.
- As with other sections, the presentation was significantly better than the corresponding document and should serve as a guideline for revising the written material.
- -- the old version of the HCAL TDR has about 122 pictures and 70 pages, after the IDRC review, we have rewrite the new version with only 30 pictures and 40 pages without the reference.

Comments in backup

HCAL

- Section 8.5 contains an extended discussion of SiPMs, mixing general background information with results from the collaboration's own R&D. This section should be streamlined to separate general background from specific experimental achievements.--.
- --this part was deleted in HCAL. The introduction of SiPM could be find in ECAL part. In the new version part, there is small **subsection 8.4.3** (Photon detector) about the SiPM, as other key technologies include in the **Secion 8.4** (Technology R&D to demonstrate technologies and prototypes).

- Since SiPMs are used extensively across the calorimeter and muon systems, it would be more effective to consolidate the discussion of SiPM R&D into a single section. This would avoid redundancy and present a more coherent overview of the topic.
- --this part was deleted in HCAL. It could be find in ECAL part **Section 7.4.2** SiPM.

Comments in backup

- Mechanical integration aspects, currently occupying much of Section 8.7, could be better placed within a general "Detector Integration" section. The authors should use their judgment to decide which integration details are most relevant to retain in the specific HCAL section, while moving broader topics to a centralized discussion.
- --there is the new section about the mechanical part at the begin of the HCAL as 8.2 Design part. The Outline of the HCAL part are the same an other Detector, first the design, then the Key technologies, both the major challenges and the R&D results. Then the simulation and performance. The Alternative HCAL options are to be a special section to overview the other group's work for the HCAL.

8 Hadron calorimeter
- 8.1 Physics Requirements of HCAL
- 8.2 Technical Survey of HCAL
- 8.3 Design of the GS-HCAL
- 8.4 Glass Scintillator
- 8.5 SiPMs for HCAL
- 8.6 Electronics & DAQ
- 8.7 Mechanics
- 8.8 Calibration
- 8.9 Performance
- 8.10 Cost
- 8.11 Outlook
- References

→

8 Hadronic Calorimeter
- 8.1 Overview
- 8.2 HCAL Design
- 8.3 Key Technologies and Major Challenges
- 8.4 Technology Development and Prototyping
- 8.5 Simulation and Performance
- 8.6 Alternative HCAL Option
- 8.7 Summary and Future Plan
- References

Comments on Draft v0.4

- General comment
- Let us first congratulate them for the huge amount of interesting work that is presented. As already observed for the Eca part also the HCal part has been restructured. It also presents directly the design choice and comments on alternatives at the end of the chapter, meeting therefore a comment made during the review in April. In the following a few high level comments and a non-exhaustive list of line-by-line comments. An annotated pdf file of the HCal put has been put at the disposal of the project members.

Comments on Draft v0.4

- High-level comments
  - Still the main problem is that a technology is proposed that is at the very beginning of the R&D cycle
    - From our point of view It will take at least five years with full resources before this calorimeter will reach the TDR level
    - We note however that the authors show awareness of this (major) shortcoming
    - The project matches perfectly a strategic R&D topic in DRD Calo but is too early for a TDR.

--The answer from Imad.

1） several components of the is technology are similar to ones used in the AHCAL technology like SiPM and readout systems as well as calibration techniques. All this is integrated in the new technology

2） although future extensive tests will confirm it, the simulation used to produce the TDR results seems to be corroborated by the first beam tests and cosmic benches.

3) the strong collaboration with local industries allow us to be confident that new generation of scintillanting glass will provide even higher performances in terms of light yield and attenuation length leading to even much better performances than the ones put in the TDR.

- **--The answer from Hengne & Sen.**
- Agree. In deed we well accept this glass scintillator technoligy is still at its early stage . however, given it's valuable potential (e.g. cheap, easy modeling, etc.) we chooose to boost it in the future CEPC HCAL application. For this reason We did the following updates in the text accordingly:
- 1.Updated the preamble part before "Overview" Section, explicitly mention that we fully aware the GS technology is at its early stage and still need at least 5 years of R&D to be a TDR-Level technology.
- 2.Update corresponding sections, to clearly present what R&D have been done, what haven't yet. And trying to make a clear and solid plan towards a mature technology at the time scale of 5 - 10 years, i.e. before the construction of the CPEC detector.

Comments on Draft v0.4

■ High-level comments

○ How critical is the non availability of CERN (i.e. a high energetic hadron beam) between the middle of 2026 and ~2029.

---May be in KEK or the Proton beam in CSNS in China.

-- A clear proposal of using CERN high energy hadron test beams for the R&D of the GS-HCAL is presented.

• The document lacks a clear plan toward construction

--please see the **section 8.4.8** Prototype, the **section 8.7** Summary and Future Plan.

The GS-HCAL development follows an aggressive yet realistic timeline:

- **2024–2025**: Finalize $40 \times 40 \times 10\,\text{mm}^3$ glass tile design and initiate mass production of 10,000 prototype tiles;
- **2026**: Complete $0.6\,\text{m}^3$ prototype assembly (8,112 tiles) and begin beam tests at CSNS or CERN;
- **2027**: Full-scale module integration and performance validation with cosmic-ray/beam tests.

Comments on Draft v0.4

- High-level comments
  - What are design parameters (on e.g. cell S/N) of the system?

-- we are expecting a 10% of MIP value as the S/N cut threshold.

  - At the moment only a handful of tiles have been tested
    - How to ensure mass production?
    - In this context how to ensure homogenous tiles and what are the criteria?

--No matter what. We must trust the production capabilities and quality control of Chinese enterprises.

--the successfull example is the 20 inch MCP-PMT for JUNO. We get the small number of prototypes at Lab in 2015, and the factory setup the mass production line in 2016, and start the mass production from 2017 to 2020, finished 15000 pics 20 inch MCP-PMTs for JUNO.

--for the Glass Scintiallator and SiPM, the situation right now are really much better than the PMTs at that time. When the CEPC will be supported by the goverment, the factories will do the mass production by themeslves.

--for the SiPM, the chinese company ZJGD (www.zjgd.com.cn) has already finished the mass production line on June 2025, and produce the SiPM with 40% PDE and acceptiable price. **The news will be publish in The Innovation will introduce it.**

A significant breakthrough achieved in the production of high-performance SiPMs with epitaxial quenching resistors

S. Qian[a,b,c,*], P. Hu[d], Z. Liu[e], J.F. Han[f], X.L. Wang[g,h]

[a] *Institute of High Energy Physics, Chinese Academy of Sciences, Beijing, 100049, China.*
[b] *State Key Laboratory of Particle Detection and Electronics, Beijing, 100049, China.*
[c] *Key Laboratory of In-fiber Integrated Optics, Ministry Education of China, Harbin Engineering University, Harbin 150001, China*
[d] *China Nuclear (Beijing) Nuclear Instrument CO.,LTD, Beijing, 100176, China.*
[e] *Paul C. Lauterbur Research Center for Biomedical Imaging, Shenzhen Institutes of Advanced Technology, Chinese Academy of Sciences, Shenzhen 518055, China*
[f] *Key Laboratory of Radiation Physics and Technology of the Ministry of Education, Institute of Nuclear Science and Technology, Sichuan University, Chengdu, 610064, China.*
[g] *Key Laboratory of Nuclear Physics and Ion-beam Application (MOE), Fudan University, Shanghai, 200443, China*
[h] *Institute of Modern Physics, Fudan University, Shanghai, 200443, China*

1. News

Recently, a significant breakthrough has been achieved in the production of high-performance Silicon Photomultipliers (SiPMs) with epitaxial quenching resistors (EQR) [1]. The EQR SiPM packaging production line, developed by CGN Capital Photonics Technology (Tianjin) Co., Ltd., has been successfully launched with a product yield exceeding 90%. This breakthrough has sparked new growth in China's semiconductor optoelectronic device industry.

The SiPM is a solid-state photon detector known for its high sensitivity and compact structure. It is a silicon chip that is composed of a series of miniature avalanche photodiodes (APDs), each operating in Geiger mode by being reverse-biased above the breakdown voltage to realize the avalanche multiplication of photoelectrons. A special resistor is connected with each

*Corresponding author.
Email address: qians@ihep.ac.cn (S. Qian)

Preprint submitted to Innovation *August 10, 2025*

GS Cell Batch Test Results --20250810

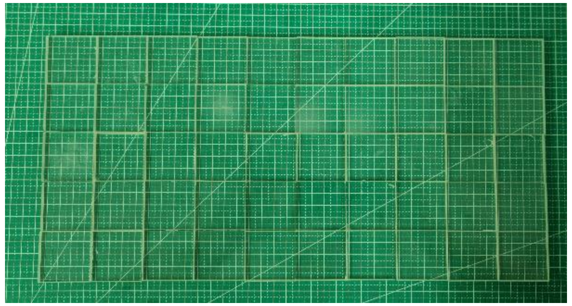
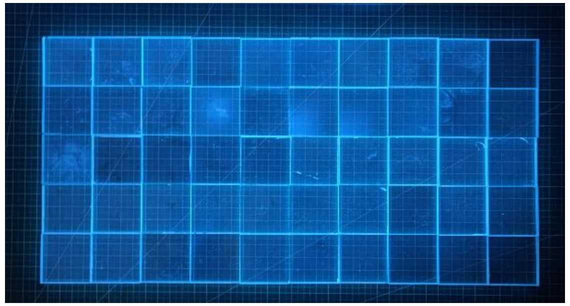

BGRI

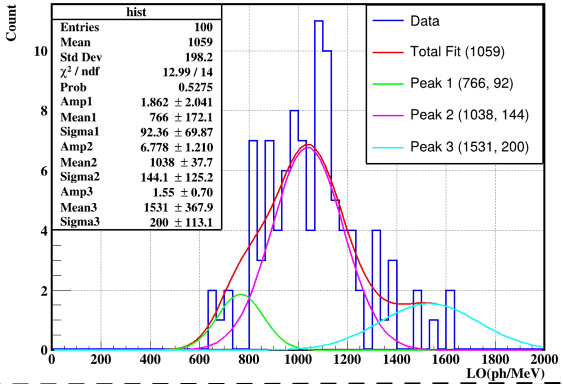

- The light output of 60.0% of GS is ⩾1000 ph/MeV (60/100)
- The light output of 21.0% of GS is ⩾1200 ph/MeV (21/100)

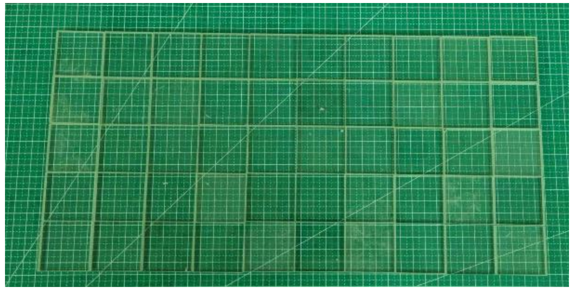
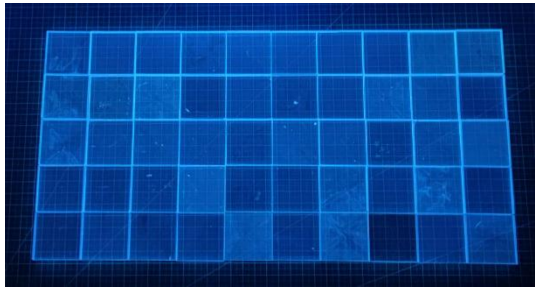

SIOM

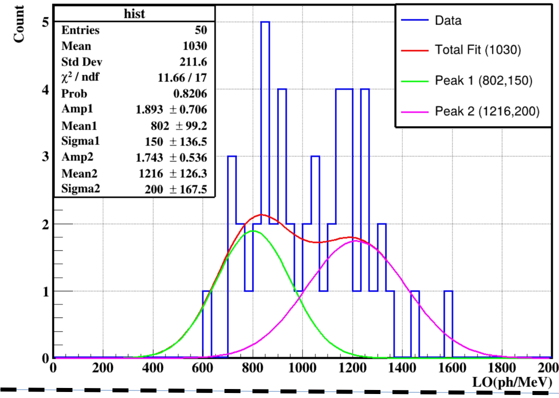

- The light output of 54.0% of GS is ⩾1000 ph/MeV (27/50)
- The light output of 20% of GS is ⩾1200 ph/MeV (12/50)

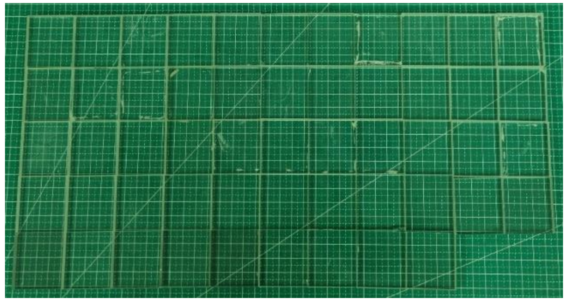
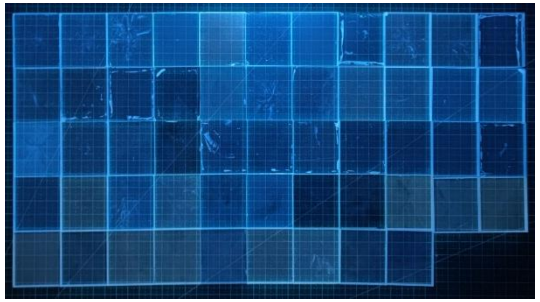

CBMA

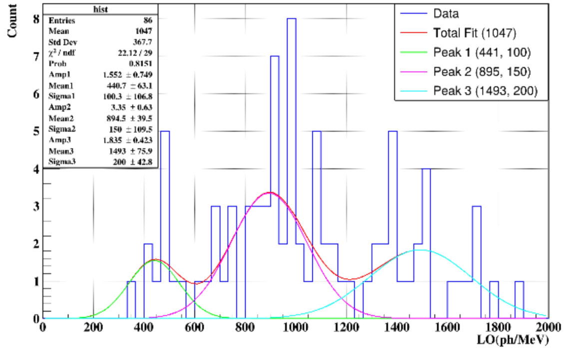

- The light output of 46.5% of GS is ⩾1000 ph/MeV (40/86)
- The light output of 31.4% of GS is ⩾1200 ph/MeV (27/86)

GS Cell Batch Test Results --20250819

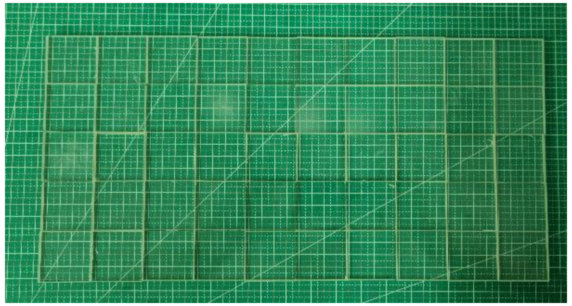
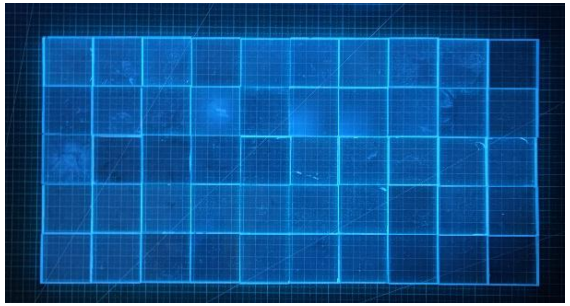

BGRI

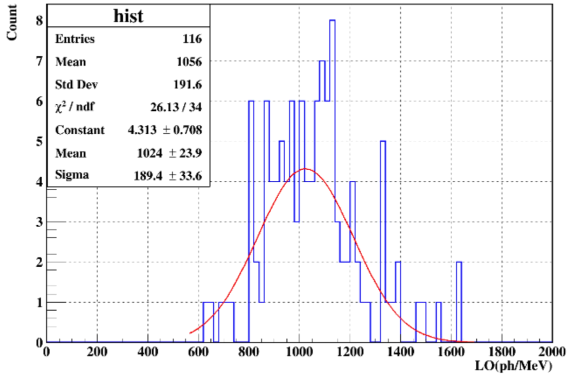

- The light output of 60.3% of GS is ⩾1000 ph/MeV (70/116)
- The light output of 20.7% of GS is ⩾1200 ph/MeV (24/116)

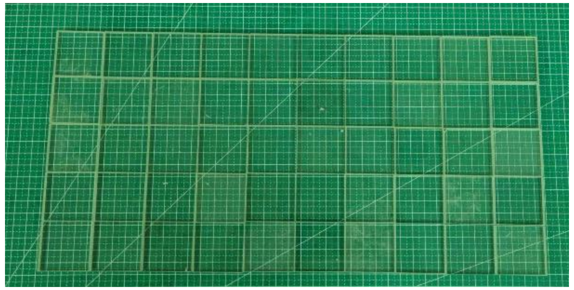
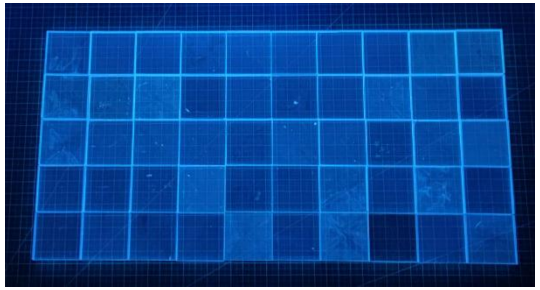

SIOM

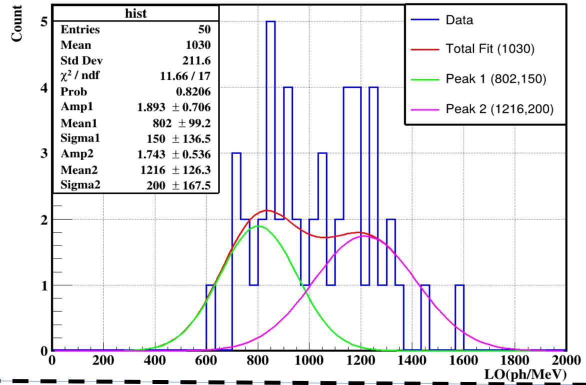

- The light output of 54.0% of GS is ⩾1000 ph/MeV (27/50)
- The light output of 24.0% of GS is ⩾1200 ph/MeV (12/50)

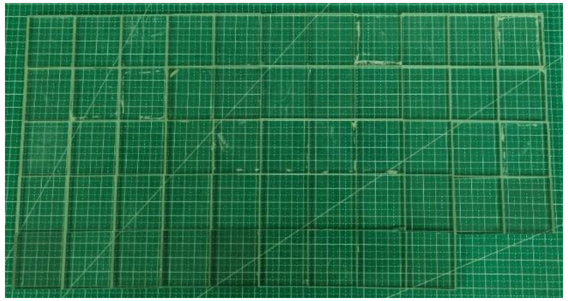
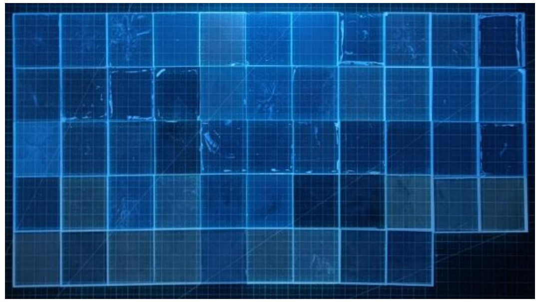

CBMA

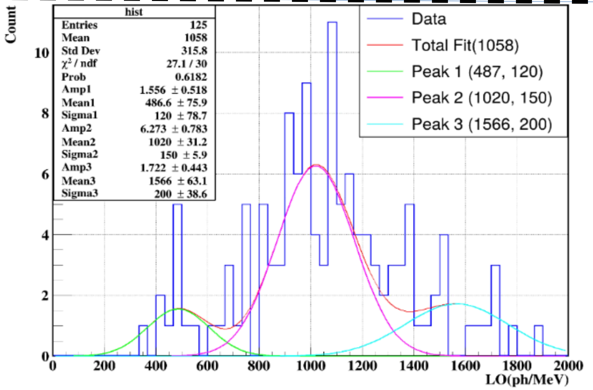

- The light output of 55.2% of GS is ⩾1000 ph/MeV (69/125)
- The light output of 30.4% of GS is ⩾1200 ph/MeV (38/125)

Comments on Draft v0.4

In the draft we don't see the results of all the (few) tiles that have been e.g. tested beam or in the cosmic stand

--In Fact， in the Section **8.4.2 Glass Scintillator**, the **Figure 8.12**: the transmission and XEL spectra of large GFO glass, the Energy spectra of GFO GS and the Scintillation decay curve of the GFO.

there is the new version for the **8.4.5 Measurements** part, the **Figure 8.17**: Measurement results of the GS cell with SiPM readout, using 137Cs radiation source and Cosmic ray.

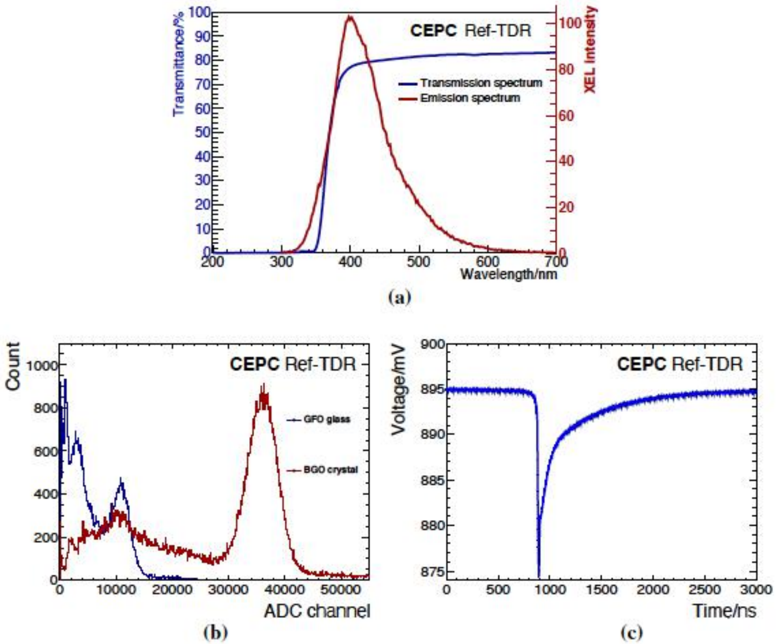

Figure 8.12: (a) Transmission and XEL spectra of large GFO glass, (b) Energy spectra of GFO GS and BGO crystal with same dimension. (c) Scintillation decay curve of the GFO glass.

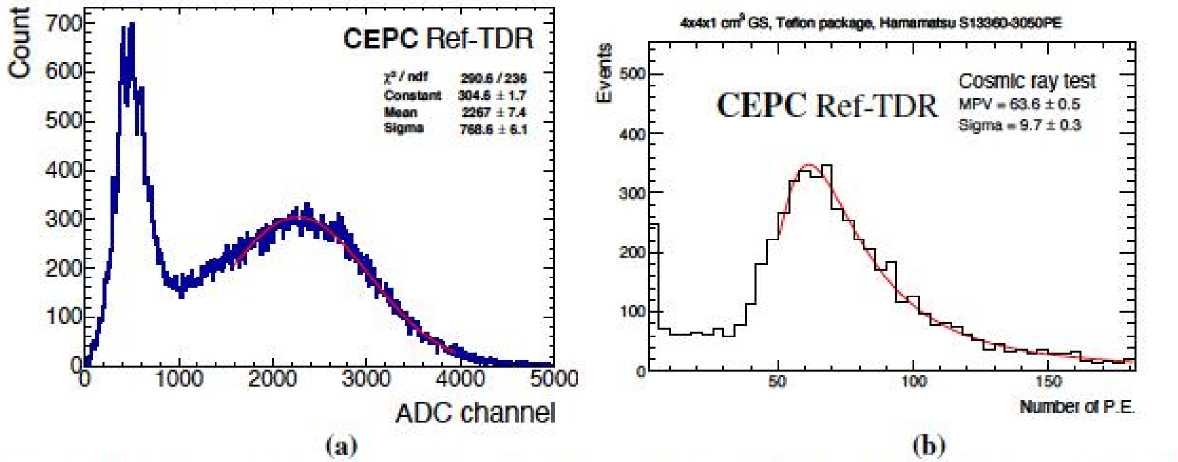

Figure 8.17: Measurement results of the GS cell with SiPM readout, the same GS cell size of $40 \times 40 \times 10$ mm^3 is used. (a) The measured ADC spectrum of GS cell with a SiPM (HPK S14160-3050HS) using ^{137}Cs radiation source. (b) Cosmic ray test results measured using HPK S13360-3050PE SiPM, resulting a light output about of 64 p.e./MIP.

Comments on Draft v0.4

- There are inconsistencies; examples (non exhaustive)
  - All SiPM tests in 8.4.4 were carried out with HPK SiPMs however for the prototype NDL SiPMs will be used

  --all changed, not fix the SiPM for HCAL.

  - Is the pre-amp tested in Sec. 8.4.6 the same that will be used in SIPAC?

  --not yet. The pre-amp was combined in ASIC, which has not designed for using right now.

- On Page 290 the authors raise concerns about the radiation hardness.
  - The tiles will not withstand 10 years of operation. Is this a fundamental problem and if yes how will this be systematically addressed?

-- radiation section is removed. it is not an issue. According to the existing TDR data, during the 10-year Higgs run (with a luminosity of 8×10^{34} $cm^{-2}s^{-1}$), the irradiation dose reaches 100 Gy.For the Z run, the luminosity is 192×10^{34} $cm^{-2}s^{-1}$, so a rough estimate suggests that 1 year of Z running would result in an irradiation dose of 240 Gy. However, since the Z-peak energy is 91 GeV (lower than the Higgs production energy), **the actual dose is expected to be somewhat lower.**

indeed, you correctly pointed out adiation hardnes is not a fundamental problem. Previously we spent many text discussing radiation damage but in fact it is not really an issue. We have receved comments from several experts that the radiation damage is actually not an issue in electron-positrom machine such as CEPC, we agree on that and re-evaluated the situation, we deceided to remove a large fraction of the radiation damage discussion.

-- from 8.4.2.3 Radiation Tolerance

Comments on Draft v0.4

The description of the cooling system (Page 279) is insufficient.

-- agree, adding more text and a figure to better describe the cooling system. More detialed could be seen in Section 8.2.2 Barrel and Section 8.2.3 Endcap.

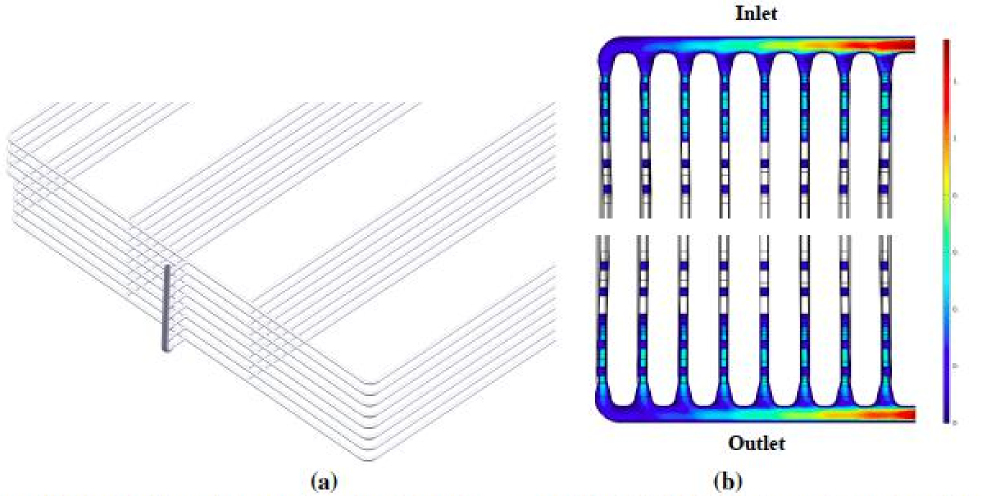

Figure 8.6: Cooling pipe routing for a barrel sector of the GS-HCAL. (a) Schematic of the eight-in-one pipeline design. (b) Simulated flow velocity (m/s) distribution of the coolant along the pipeline, with inlet and outlet positions indicated.

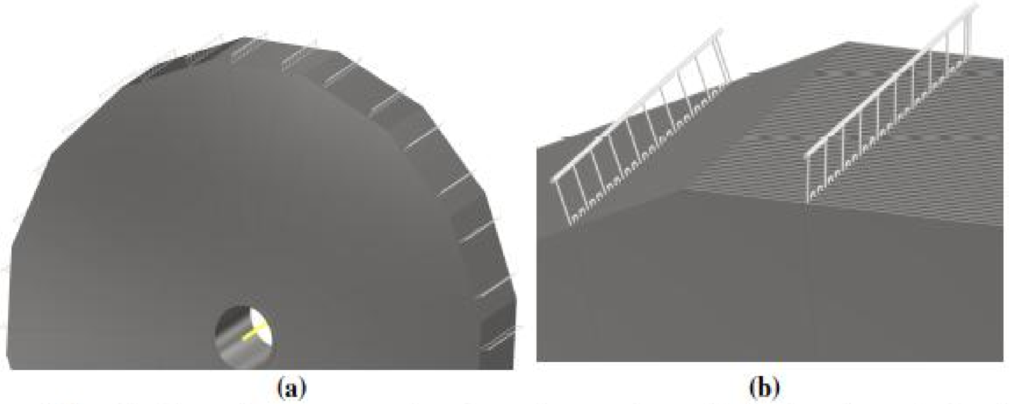

Figure 8.8: Cooling pipe structure for the endcap, where (a) is showing a half of the endcap, and (b) is showing a zoomed in corner of the endcap.

Comments on Draft v0.4

- Think to shorten the introduction to 8.4
- ——The Part 8.4 have to change as follows：
- keep the 8.4.1 Historical review； 8.4.3 Photon detector； 8.4.4 Simulation Study of Attenuation Length

  8.4.6 Calibration；8.4.7 Readout electronics for R&D； 8.4.8 Prototype

- rename 8.4.5 Measurements of GS with SiPM as 8.4.5 Measurements

- **rewrite the 8.4.2 Glass scintillator；**

  8.4.2.1 Light Yield,

  8.4.2.2 Light Attenuation Length；

  8.4.2.3 Radiation Tolerance

- **rewrite the 8.4.2 Glass scintillator；（1）light yied，**
- delate the result of the electron beam result；
- remove cosmic ray test result to 8.4.5 Measurement

8.4.2.1 Light Yield

Figure 8.11 shows the pictures of GFO glasses with a size of $40 \times 40 \times 10\ mm^3$ under natural (such as regular room light) and ultraviolet light. Figure 8.12(a) shows the X-Ray Excited Luminescence (XEL) spectrum and transmission spectrum of a GFO glass,The transmittance in the visible light range exceeds 80%. Combined with the XEL spectrum, it can be observed that there is a certain self-absorption effect in the glass [20]. Additionally, as the glass thickness increases, its transmittance in the visible spectrum decreases from approximately 80% to around 75%. The measurable light output of GFO glass is a critical factor for HCAL applications. Extensive γ-ray testing has demonstrated that the light yield of GFO glasses can consistently exceed 1000 ph/MeV. When measured with an XP2020 (2 inch) Photomultiplier Tube (PMT), the detected photo-electron number reaches 1/3 that of BGO crystals with identical dimensions [21], as shown in Figure 8.12(b). Figure 8.12(c) presents the scintillation decay profile of GFO glass under γ-ray excitation. While maintaining a light yield of 1000 ph/MeV, the decay time of the slow component can be controlled to below 500 ns. Although achieving faster decay time remains challenging, the large-scale GFO glass successfully maintains an optimal balance between density, light yield, and scintillation decay characteristics.

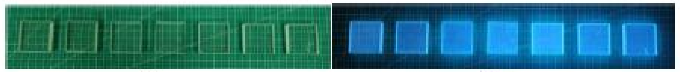

(a) (b)

Figure 8.11: GFO glass cells with the size of $40 \times 40 \times 10\ mm^3$ under (a) natural light and (b) ultraviolet light.

To verify the performance stability of the GS, a batch of 150 glass samples were produced, and corresponding performance tests were conducted. Additionally, the radiation resistance characteristics of GFO glass under proton and γ-ray irradiation were tested. With proton beam irradiation at 800 Gy, the 400 nm transmittance showed a 60% reduction from its original value, the cumulative reduction further arrived at 87% for a dose of 8100 Gy. While for light yield, when the dose reached 400 Gy, it decreased to 34% of its original value [22]. The light yield dropped to 71% under γ-ray irradiation of 100 Gy, corresponding to ten years of data taking of the CEPC GS-HCAL.

Figure 8.8: DESY electron beam test of the GFO glass tiles in 2023. Left figure shows the experimental setup, right figure shows the measured p.e. distribution.

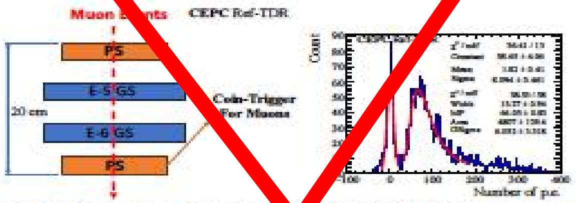

Figure 8.9: IHEP cosmic ray setup performed in 2024 of GFO glass tiles (left), and the measured p.e. distributions for MIPs (right).

To independently validate the MIP response, a second measurement was performed using cosmic muons in a vertical stack configuration at IHEP in 2024. Two Plastic Scintillator (PS) paddles provide coincidence triggers above and below the GS tiles (labeled E-5 and E-6) to ensure clean muon tracks. This setup is schematically shown in the left panel of Figure 8.9. The readout is using Hamamatsu S13360-6025CS SiPM. A longer integral gate of 4 μs was employed to fully collect the slower scintillation components. The measured MIP response for the E-5 tile reached an MPV of approximately 67 p.e./MIP, corresponding to an inferred light yield of ~750 photons/MeV, which is consistence with the DESY results.

Both measurements confirm the feasibility of using GS tiles for high-granularity HCAL applications. A summary of the results is presented in Table 8.4. These results validate the promising performance of GS tiles and provide critical input for optimizing the calorimeter design for CEPC.

Table 8.4: Summary of GS tile beam test and cosmic ray measurements.

Test Setup	Integral Gate	Light Yield	MIP Response
DESY Electron Beam	1 μs	600–700 ph/MeV	90–100 p.e./MIP
IHEP Cosmic Ray (E-5)	4 μs	~750 ph/MeV	65–70 p.e./MIP

- rewrite the 8.4.2 Glass scintillator； (2) Light attenuation length，
- delate the test result of the data by the light output in our lab published in Ref[18]；
- retest the samples by the transmittance data and give the new results and also the ref.23

R. Y. Zhu et al. "A Study on the properties of lead tungstate crystals". Nucl. Instrum. Meth. A 376 7517 (1996), pp. 319-334..

Light attenuation length

The attenuation length (L_0) is a critical parameter for evaluating light transmission performance in scintillators. Multiple batches of GFO glass samples with cross-sectional dimensions of 5 × 5 mm^2 and thicknesses ranging from 1–15 mm were prepared for systematic measurements (Fig. 8.10). The best-performing GFO glass sample currently available achieves an attenuation length of 6.2 cm at 400 nm. This value is used as the standard reference in the TDR, and all performance results are based on it.

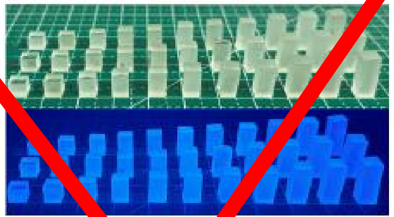

Figure 8.10: GFO glass samples under natural light (top) and ultraviolet light (bottom).

The light attenuation follows the exponential relation is given by $Y = Y_0 \cdot \exp(L/L_0)$, where Y_0 is the initial photon yield, Y the yield after propagation distance L, and L_0 the characteristic attenuation length. Initial measurements yielded $L_0 = 2.3 \pm 0.01$ cm [18], limited by glass matrix defects and Ce^{3+} self-absorption.

Through process optimization, the light yield of GFO glass increased from 1000 to over 1500 ph/MeV, suggesting corresponding attenuation length improvements. Figure 8.11 (a) illustrates the γ-ray spectral method for determining the light attenuation length. The method involves measuring the ratio of the initial light yield (Y_0) to the light yield after transmission through varying glass thicknesses (Y). By fitting this ratio as a function of thickness, we extract the attenuation length, yielding a value of $L_0 = 2.3$ cm and $L_0 = 3.4$ cm for two batches of glass samples before and after optimization, respectively.

A more accurate method determines L_0 through thickness-dependent transmittance (T) can be written as $L_0 = (L_2 - L_1)/\ln(T_{L_1}/T_{L_2})$, where T_L is the transmittance at thickness L. This method accounts for full-volume light penetration, eliminating position uncertainty. Figure 8.11 (b) shows the improved attenuation length of 6.2 cm at 400 nm (emission peak), with consistent 5.8–6.2 cm performance across the visible spectrum - a 100% improvement over previous samples (3.1 cm at 400 nm). These results confirm that γ-ray methods systematically underestimate L_0, while verifying GFO's about 6 cm attenuation length enables efficient light collection.

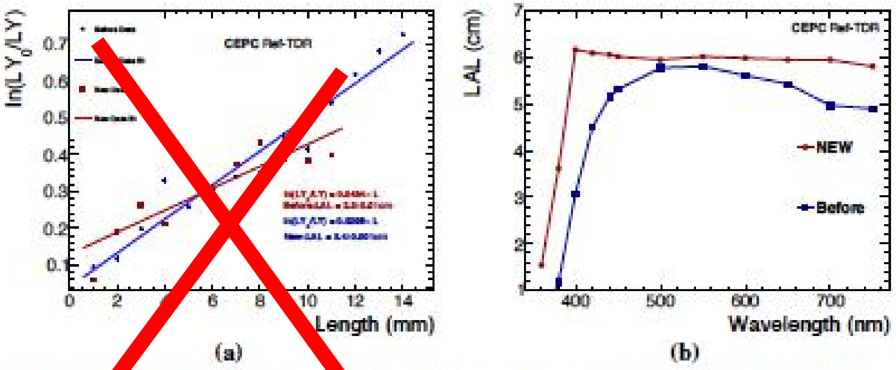

Figure 8.11: (a) Light yield ratio $\ln(Y_0/Y)$ as a function of the thickness of the glass is fitted to extract light attenuation length (LAL). (b) Attenuation length spectrum from transmittance measurements ("New": current GFO; "Before": previous samples).

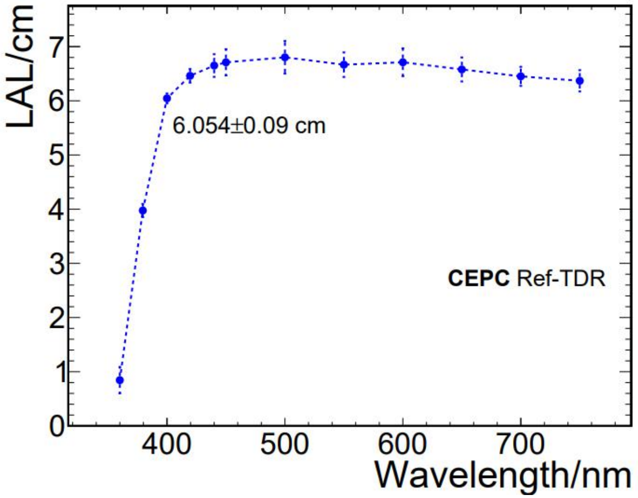

- rewrite the 8.4.2 Glass scintillator； (3) Radiation resistance ，
- just delate this part and give the result in (1) Light Yield part. and ref the papaer published in NIMA about this result right now (suggested by Imad).
- **Ref [22]** S.H. Yin et al. "Radiation resistance study of Gd-Al-B-Si-Ce3+ glass scintillators using 80MeV proton beam irradiation". Nucl. Instrum. Meth. A 1081 (2026), p. 170869. issn: 0168-9002.

Radiation resistance

The radiation resistance of glass scintillators is crucial as their performance degrades after irradiation. The GFO glass samples were studied using an 80 MeV proton beam at the Associated Proton Beam Experiment Platform (APEP) [19] across a wide dose range (400 Gy to 4.1×10^4 Gy). Proton flux for this test is 4.86×10^9 (p/cm²/s), and the beam spot size is 50×50 mm². Seven $10\times10\times10$ mm³ pieces (labeled #1–#7) were used for this test, using different radiation time to obtain corresponding radiation dosage as shown in Table 8.5). Sample #1 kept as an unirradiated reference.

The scintillation properties were characterized through transmission spectra, XEL, light output, and decay time measurements (Table 8.5). Unirradiated sample showed 78% transmittance at 400 nm, while transmittance of irradiated samples dropped to 31% with a dose of 800 Gy, and further dropped to 10% for a dose of 8100 Gy, consistent with visible color changes indicating defect formation. The Ce^{3+} emission peak (386 nm in unirradiated samples) shifted slightly to 376–384 nm after irradiation. Figure 8.12 displays the visual changes in samples #1 to #7 under progressively higher radiation doses, with increased dosage correlating to decreased transparency and darker color.

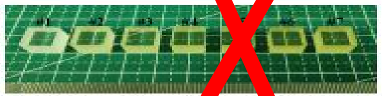

Figure 8.12: The photograph of proton beam irradiated glass samples. From sample #1 to #7, the radiation dosage progressively increases, resulting in darker color with decreased transparency.

In contrast to proton irradiation, gamma irradiation tests evaluate performance degra-

16

Draft v0.3.1

8.4 Technology R&D to demonstrate technologies and prototypes

Table 8.5: Performance summary of the glass tiles after proton irradiation test.

Sample	Dose (Gy)	Transmittance @ 400 nm (%)	XEL (nm)	Light Output (ph/MeV)	Decay Time (τ) (ns)
#1	0	77.9	386	552	87, 985
#2	400	37.4	376	187	89, 980
#3	800	31.3	380	–	–
#4	2000	13.7	384	–	–
#5	4100	10.4	376	–	–
#6	8100	8.3	380	–	–
#7	41000	5.8	376	–	–

dation at lower doses (10–400 Gy). A ^{60}Co point source (3.656×10^{11} Bq) was used, emitting gamma rays at 1.1732 MeV and 1.3325 MeV. The absorbed dose rate follows the inverse square law relative to the source distance. Six $5\times5\times5$ mm³ glass samples were irradiated simultaneously for 37.5 hours at varying distances (10–63 cm) to achieve different dose rates, slight yellowing (darkening in color) for samples with higher radiation dosage can be observed.

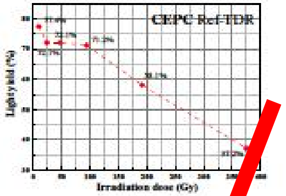

Figure 8.13: Gamma irradiation results showing the relative light yield of the scintillator as a function of irradiation dose. The light yield decreases gradually with increasing dose, reaching 71.2% at 100 Gy.

Scintillation performance was characterized through transmission spectra, XEL, light output, and decay time measurements. The maximum transmittance degradation was 14% - significantly less severe than proton irradiation at comparable doses (400 Gy). This difference likely stems from the lower dose rate and reduced ionization damage in gamma irradiation, as protons have higher linear energy transfer. The emission peaks remained stable (380-386 nm), consistent with proton irradiation results. Light output measurements using the same ^{137}Cs/PMT setup showed progressive degradation: 71% retention at 100 Gy and 37% at 375 Gy, matching proton irradiation trends. Decay times exhibited minimal variation, 87-89 ns fast component, 978 ns slow component, again consistent with proton irradiation observations. The gamma irradiation test results of the scintillator samples, showing the relative light yield as a function of accumulated dose, are shown in Figure 8.13. A significant degradation in light yield is observed with increasing dose,

17

Draft v0.3.1

8.4 Technology R&D to demonstrate technologies and prototypes

with the yield dropping to about 71.2% at 100 Gy. This corresponds to an expected total dosage (about 100 Gy) of CEPC HCAL after 10 years of data taking.

The comparative analysis reveals that while both radiation types cause similar qualitative effects, gamma irradiation induces less severe degradation at equivalent doses. This suggests that the damage mechanism depends not only on total absorbed dose but also on radiation type and dose rate, with proton irradiation causing more severe ionization damage due to higher linear energy transfer.

Nuclear Instruments and Methods in Physics Research A 1081 (2026) 170869

Contents lists available at ScienceDirect

Nuclear Inst. and Methods in Physics Research, A

journal homepage: www.elsevier.com/locate/nima

Technical notes

Radiation resistance study of Gd-Al-B-Si-Ce^{3+} glass scintillators using 80 MeV proton beam irradiation

S.H. Yin [a], P. Hu [a,*], S. Qian [b,c,**], H. Cai [d], D.P. Chen [e], J.F. Han [f], D.B. He [e], C. Hu [g], Z.H. Hua [b], S.Q. Li [d], W.C. Li [e], S. Liu [h], L.S. Qin [i], J. Ren [j], Z.X. Sui [h,j], X.Y. Sun [k], G. Tang [i], Z.L. Wang [l], Y.F. Wen [k], D. Yang [h], M.H. Zhang [g], Y. Zhu [j]

[a] China Nuclear (Beijing) Nuclear Instrument CO., LTD, Beijing, 100176, China
[b] Institute of High Energy Physics, Chinese Academy of Sciences, Beijing, 100049, China
[c] State Key Laboratory of Particle Detection and Electronics, Beijing, 100049, China
[d] China building materials academy, Beijing, 100024, China
[e] Shanghai Institute of Optics and Fine Mechanics, Chinese Academy of Sciences, Shanghai, 201800, China
[f] Institute of Nuclear Science and Technology, Sichuan University, Chengdu, 610064, China
[g] Shanghai Institute of Ceramics, Chinese Academy of Sciences, Shanghai, 201899, China
[h] Beijing Glass Research Institute, Beijing, 101111, China
[i] College of Materials and Chemistry, China Jiliang University, Hangzhou, 310018, China
[j] College of Physics and Optoelectronic Engineering, Harbin Engineering University, Harbin, 150001, China
[k] Department of Physics, Jinggangshan University, Ji'an, 343009, China
[l] Research Center for Space Optical Engineering, Harbin Institute of Technology, Harbin, 150001, China

ARTICLE INFO

Keywords:
Glass scintillators
Radiation resistance
Proton beam
Scintillation performance

ABSTRACT

High-density Ce^{3+}-doped Gd-Al-B-Si glass scintillators have been developed by the Glass Scintillator R&D Collaboration (GS Collaboration) for applications in nuclear and high energy physics. One of the critical factors in these applications is the radiation resistance of the glass scintillator. The impacts of proton irradiation on Ce^{3+}-doped Gd-Al-B-Si glass samples have been investigated at doses up to approximately 4×10^4 Gy, utilizing the 80 MeV proton beam on the Associated Proton Beam Experiment Platform (APEP) located at the China Spallation Neutron Source (CSNS). The optical and scintillation properties, including emission, transmittance, light output, decay time and their degradation after proton irradiation, have been measured. Blue shifts of emission peaks were observed in X-rays excited luminescence (XEL) spectra after proton irradiation. Additionally, a red shift in the cut-off wavelength and a decrease of approximately 50% in transmittance at 400 nm were also observed after proton irradiation. The light output decreases by approximately 2/3 after 400 Gy proton irradiation, without significant alteration in the decay time constants of fast and slow components. This research serves as an important reference for evaluating the radiation resistance of high-density Gd-Al-B-Si-Ce^{3+} glass scintillators and can guide their practical applications.

1. Introduction

Over recent decades, significant progress has been made in high performance scintillation materials due to increasing demand. Among solid-state scintillators, glass scintillators distinguish themselves through tunable scintillation performance and physicochemical properties, which can be customized by modifying the glass matrix composition and dopants to meet application-specific requirements. Furthermore, glass scintillators are advantageous due to their relatively simple preparation process, low cost, excellent moldability, and scalability for mass production [1]. These features provide glass scintillators with great potential for application in various fields, including high-energy physics experiments [2–4], nuclear radiation monitoring [5,6], nuclear radiation imaging [7–9] and other fields [10,11].

In comparison to plastic and crystal scintillators, glass scintillators with high density, moderate light yield, and fast decay time present notable advantages in the design of calorimeters for large colliders, such as the CEPC (Circular Electron-Positron Collider) [12]. These properties enable excellent detection performance in a cost-effective

* Corresponding author.
** Corresponding author at: Institute of High Energy Physics, Chinese Academy of Sciences, Beijing, 100049, China.
E-mail addresses: hupeng6550575@163.com (P. Hu), qians@ihep.ac.cn (S. Qian).

Comments on Draft v0.4

- **The constant term is still an issue.**
  - Line 7867: "Both approaches led to a reduction in the fitted constant term". What was the fraction of the events that were selected?
  - We propose to show the linearity in addition to the resolution
  - Please comment on the expected e/h ratio
  - We understand "all inner sub-detectors are removed" in this study.
  - Since there will be an ECAL before the HCAL in the actual experiment, the effective depth of calorimetry will be larger and the selection and constant term (with and without selection) will be different. It is also interesting to investigate how the different responses in the ECAL and the HCAL will impact the constant term in the integrated detector.
  - The AHCAL prototype discussed in Sec. 8.6.2 has a depth (from memory) of 4-5 interaction lengths but a constant term of only 2.59%. Thus, the depth cannot be the only reason for the large constant term of the GS HCAL

-- we agree with your suggestions above, we are implementing them one by one, as you have correctly pointed out, this section have already rewriten with these comments in the new version in **Section 8.5.2** Hadron Energy Resolution and in **Section 8.5.3** Energy Response e/h Studies.

Comments on Draft v0.4

- Line-by-Line Comments
- Line 6952 - "The HCAL is a key component in achieving the jet energy resolution". One may could argue it is THE key component

--agree, indeed, Re-written the beginning of the chapter, and provided justification and discussion why HCAL is "THE key component", e.g. HCAL is responsible for the reconstruction of >70% of jet energy....etc.

- Lines 6962-6964 "plastic scintillators and gaseous detectors, with readout based on SiPMs or other photon sensors.”. This is confusing. Maybe "plastic scintillators, with readout based on SiPMs or other photon sensors, and gaseous detectors."?

--agree, fixed, Re-written the beginning of the chapter.

- Line 6983 "$W$and Zdecays" - spaces missing - "W and Z decays"

--agree, fixed, re-written the beginning of the chapter.

- Lines 7042-7043: "851.34 mm" and "1367.56mm" are unnecessarily precise (10 microns). Could this be rounded off to mm? --agree, fixed.
- Figure 8.3: "851.34 mm" and "1367.56mm" are unnecessarily precise (10 microns). Could this be rounded off to mm? --agree, fixed.
- Lines 7570-7574: Could some example distributions be shown? --Added.
- Line 8066 "measure hadronic jets energy" I believe jet should be singular. "measure hadronic jet energy" line 8068 "GS and SiPMs'. We suggest spelling these out again when first mentioned in the summary ----agree, fixed.
- Line 8082 "This can be achieved" -> may be achieved? -> "This may be achieved" -----agree, fixed.

---Agree, the pointed out parts have already update in the new version.

Comments on Draft v0.4.1 from Roman

The comments from Roman on 29th.July. 2025.

- ----all the comments are replayed one by one within the PDF file.
- <CEPC_Ref_TDR_v0.4.1_BarcelonaEdition-Roman_reply.pdf>

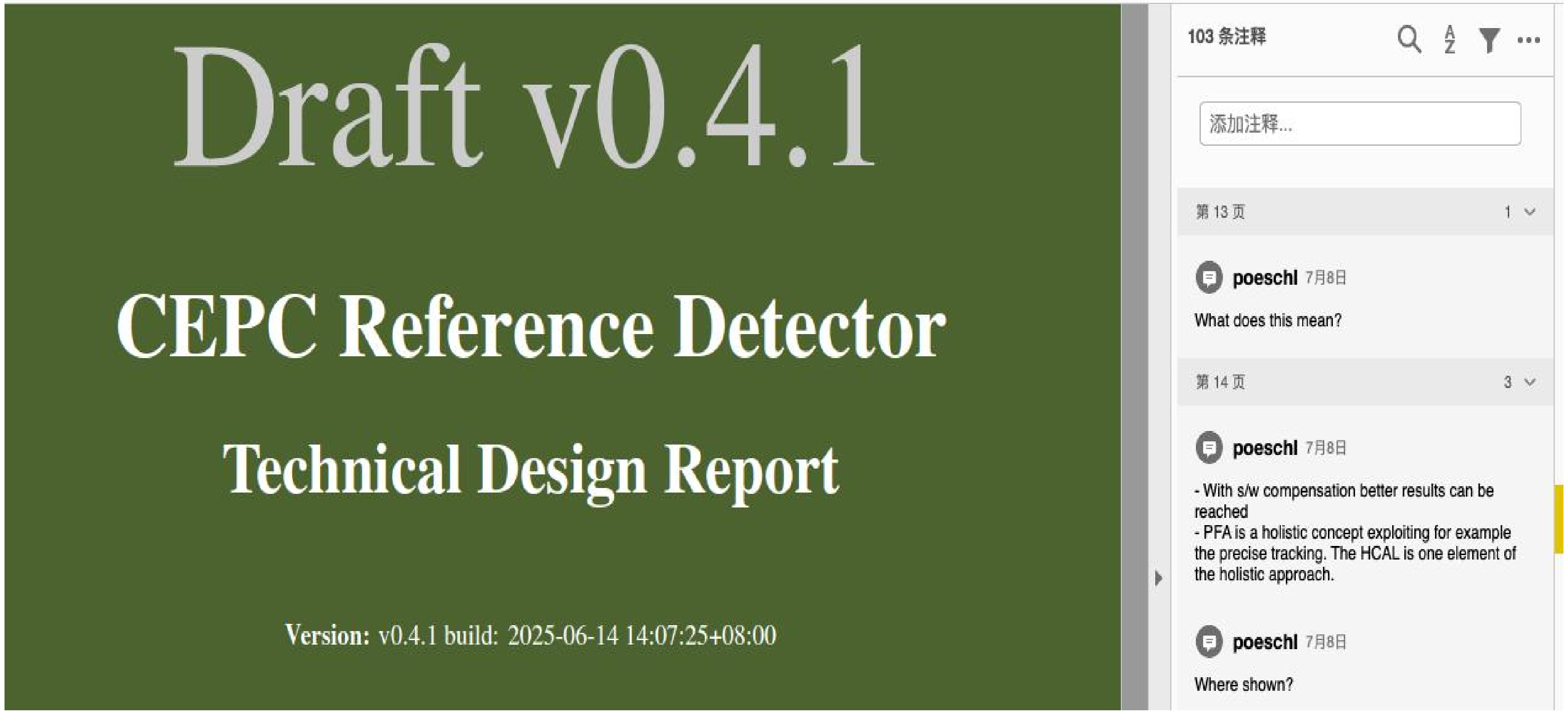

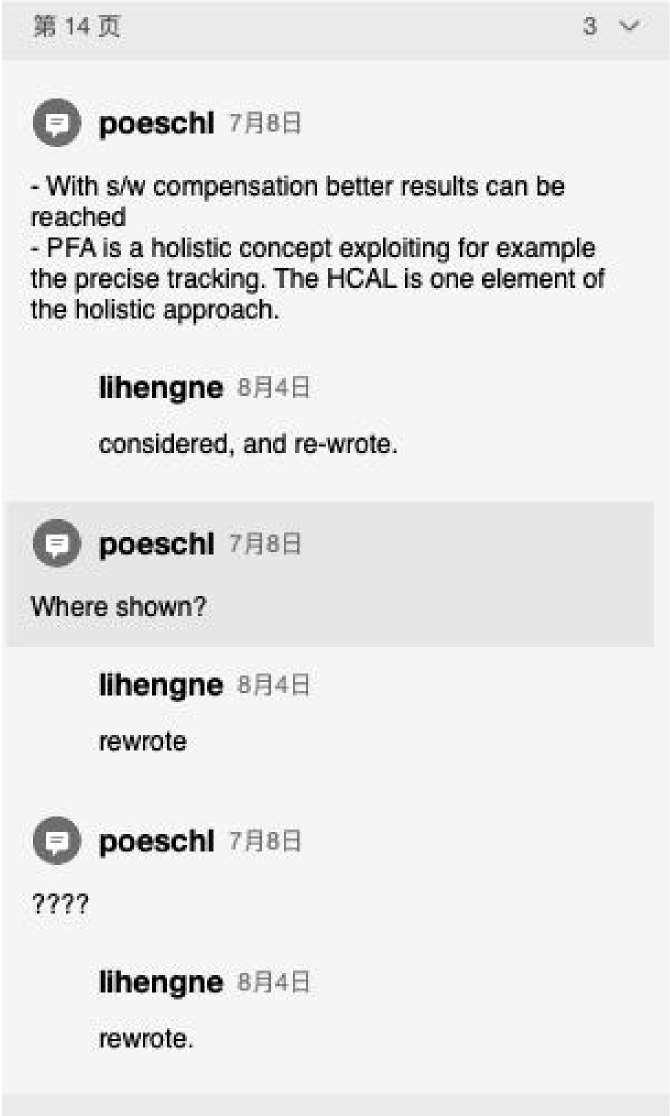

Comments on Draft v0.4.1 from Roman

Origin of four emission lines in GFO spectrum (is the multiline structure a problem?

- ----no, it's not the background noice, it is the usefull signals. They are the ADC pedestal,
- the 32keV peak,
- the 180keV peak,
- and the 662keV full-energy peak.

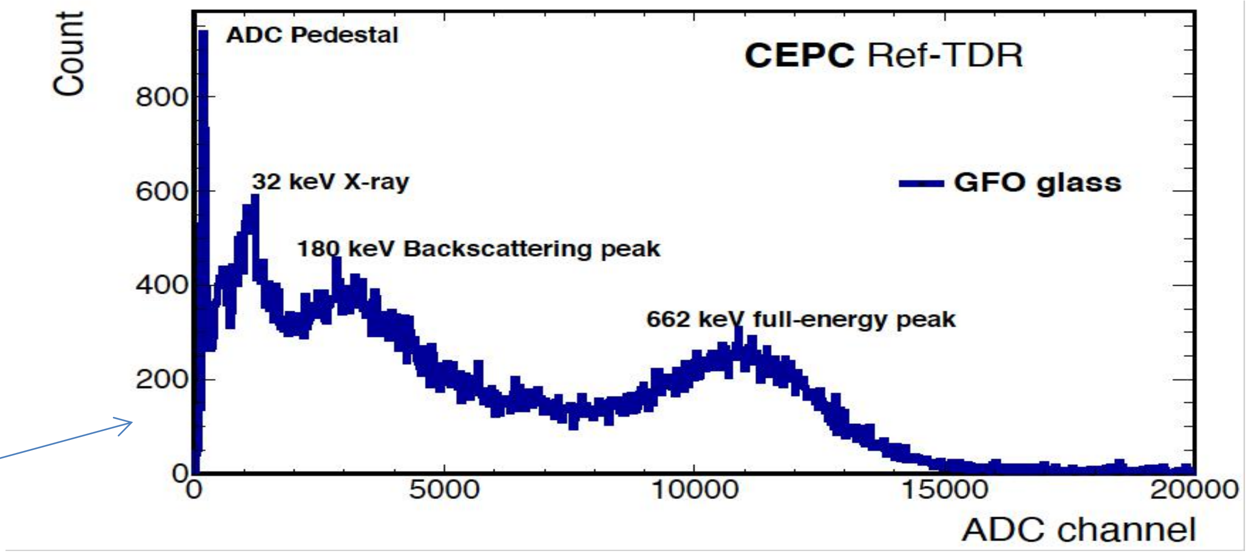

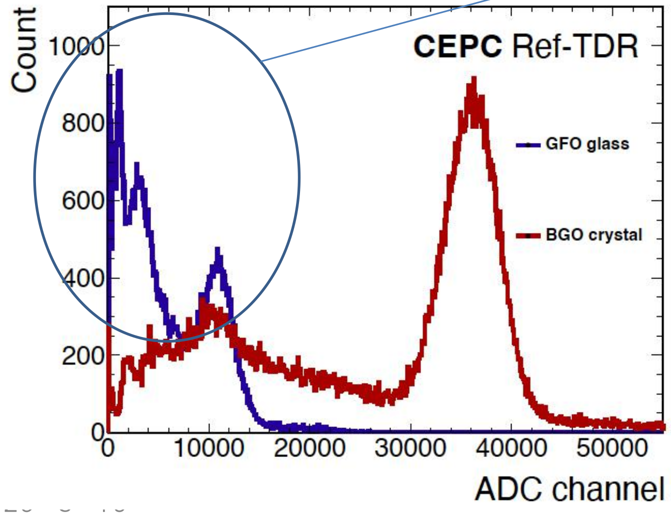

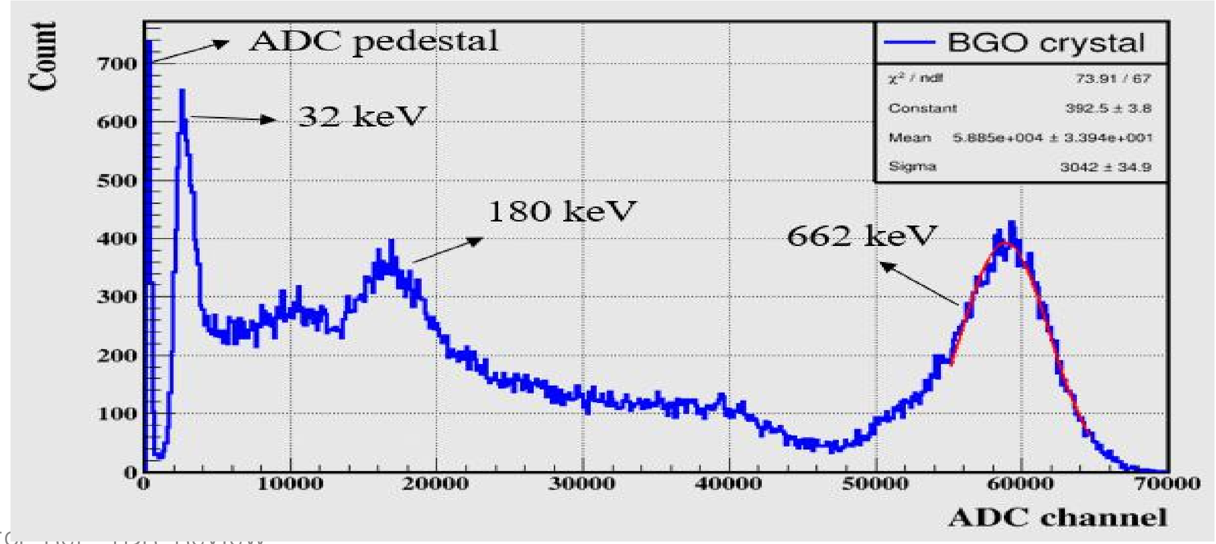

Comments on Draft v0.4

- The constant term is still an issue.
  - Line 7867: "Both approaches led to a reduction in the fitted constant term". What was the fraction of the events that were selected?

it is less than 20%, the selection requires the shower starts in the first 60mm, curresponding to the first two layers, about 0.25 nulcear interaction length, which agrees with the calculation usign the simplified formula P = 1-exp(-0.25) ~ 0.2 . Attached is the eff. (fraction of starting showin in first two layers) vs each energy points in the simulation.

the text modified to be "The other required the hadrons to initiate their first interaction within the first two layers of the \gls{GS-HCAL} (corresponding to the initial $0.25\lambda_\mathrm{I}$), though such events constituted less than 20\% of the total sample."

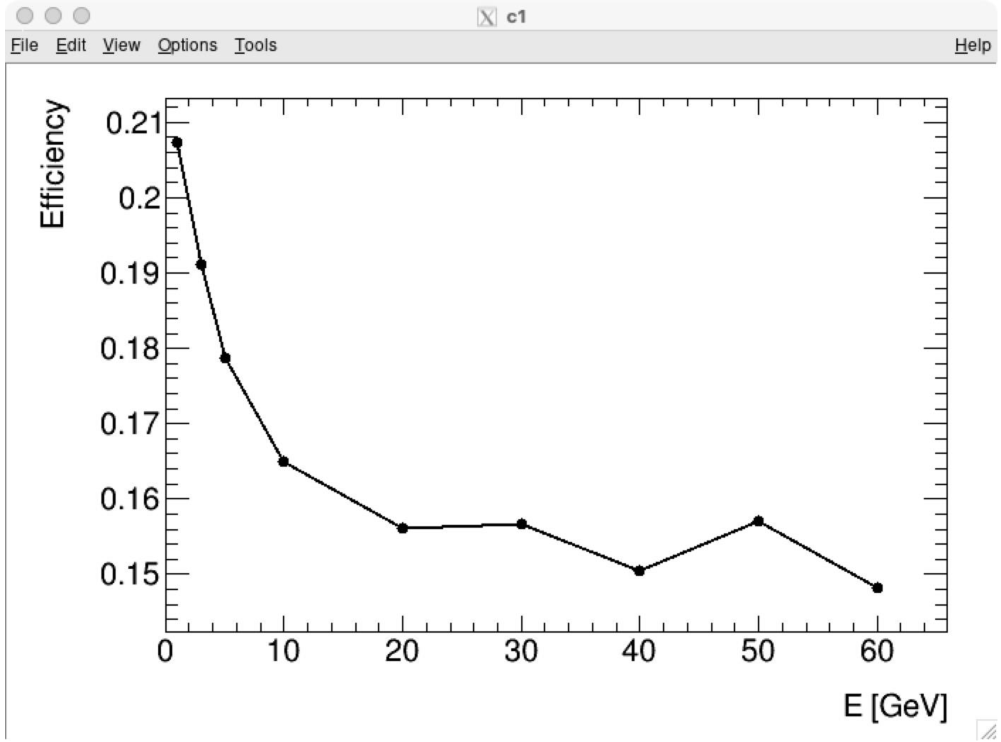

Comments on Draft v0.4

- The constant term is still an issue.
  - We propose to show the linearity in addition to the resolution

--As shown in Fig. 8.24, conparing linearity and resolution between with and without digitisation, the linearity does not show a apparent issue, i.e. the leackage, or the hadronic shower longitudinal profile is not expected to depend on the energy of the incident hadrons, e..g.

accroding to some previous studies such as [Y.A. Kulchitsky, V.B. Vinogradov/Nucl. Instr. and Meth. in Phys. Res. A 413 (1998) 484—486], where Longitudinal profiles of the hadron showers of 20 GeV (crosses), 50 GeV (squares), 100 GeV (open circles) and 140 GeV (triangles) energies as a function of the longitudinal coordinate x in units j

I for the conventional iron-scintillator calorimeter do not show apparent difference in the shape.

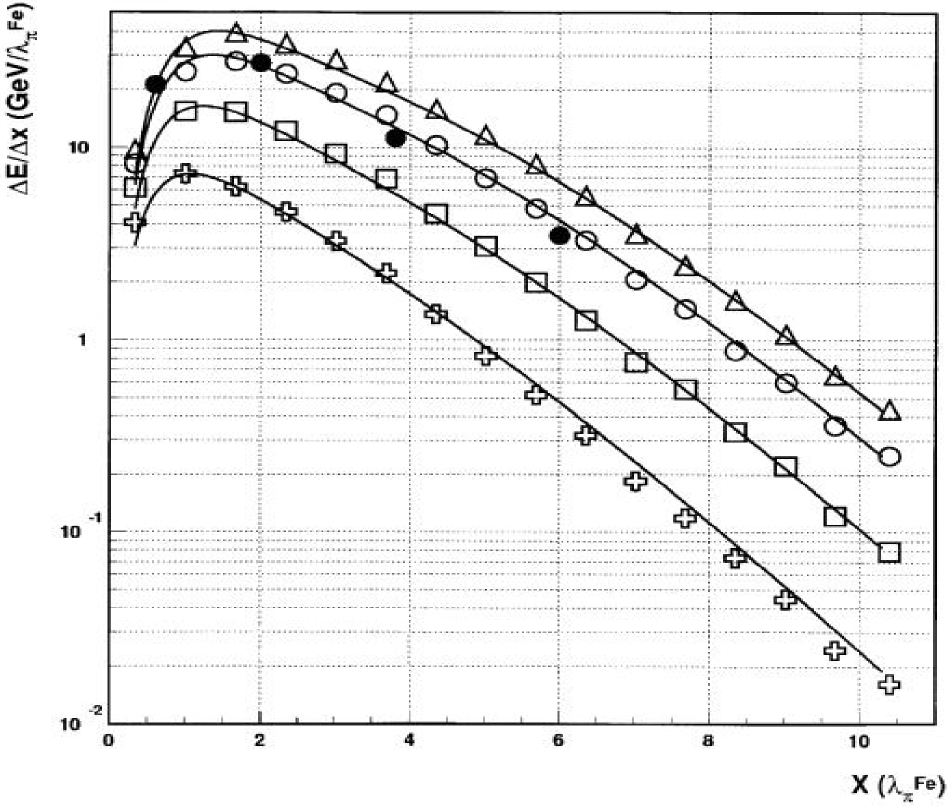

Fig. 1. Longitudinal profiles of the hadron showers of 20 GeV (crosses), 50 GeV (squares), 100 GeV (open circles) and 140 GeV (triangles) energies as a function of the longitudinal coordinate x in units λ_I for the conventional iron-scintillator calorimeter [4] and of 100 GeV (black circles) for the tile iron-scintillator calorimeter [8]. The solid lines are calculations by function (3) with parameters from Ref. [4].

Comments on Draft v0.4

- The constant term is still an issue.
  - Please comment on the expected e/h ratio

--We added a new subsection based on previous samples describing e/h results " 8.5.3 Energy Response e/h Studies."

By fitting the energy responses of electron and pion, kion...etc, the e/h is derived to be from 1.02 to 1.14, exhibits a non-compensation at the level of 9–14%,

  - We understand "all inner sub-detectors are removed" in this study.

-- indeed, added this information in the following setence in the pretty beginning of this section. :

“In initial studies of the \gls{GS-HCAL}, the energy resolution yielded a constant term (\$b\$) of approximately 5–6\% based on Geant4 full simulations with all inner sub-detectors (e.g., \gls{ECAL}) removed. ”

Comments on Draft v0.4

- The constant term is still an issue.
  - Since there will be an ECAL before the HCAL in the actual experiment, the effective depth of calorimetry will be larger and the selection and constant term (with and without selection) will be different. It is also interesting to investigate how the different responses in the ECAL and the HCAL will impact the constant term in the integrated detector.

-- Indeed, agree, with the ECAL infront of HCAL the overall ECAL+HCAL PFA results will largely reduce the impact of the leagage, and therefore smaller constent term. A through study is needed as the next step after TDR, but we already added this point here:

"As mentioned before, the leakage studies were performed with \gls{HCAL}-only. In the full \gls{CEPC} detector configuration, the \gls{ECAL} with about $1.2\lambda_\mathrm{I}$ will cause approximately 70\% of hadrons to initiate showers before reaching the \gls{GS-HCAL}.

This upstream shower development is expected to significantly reduce leakage effects and consequently lower the constant term in the combined \gls{ECAL} and \gls{HCAL} system."

  - The AHCAL prototype discussed in Sec. 8.6.2 has a depth (from memory) of 4-5 interaction lengths but a constant term of only 2.59%. Thus, the depth cannot be the only reason for the large constant term of the GS HCAL

--After verify this point we learned that the beam test results onf the AHCAL prototype showing 2.59% constant term is after a selection of events showing interactions (with energy deposition) in the first several layers to keep sufficient containment in the AHCAL, and avoid leakage from the back.